STATE OF ALASKA
DEPARTMENT OF NATURAL RESOURCES

SHORT NOTES ON ALASKAN GEOLOGY
1982-83

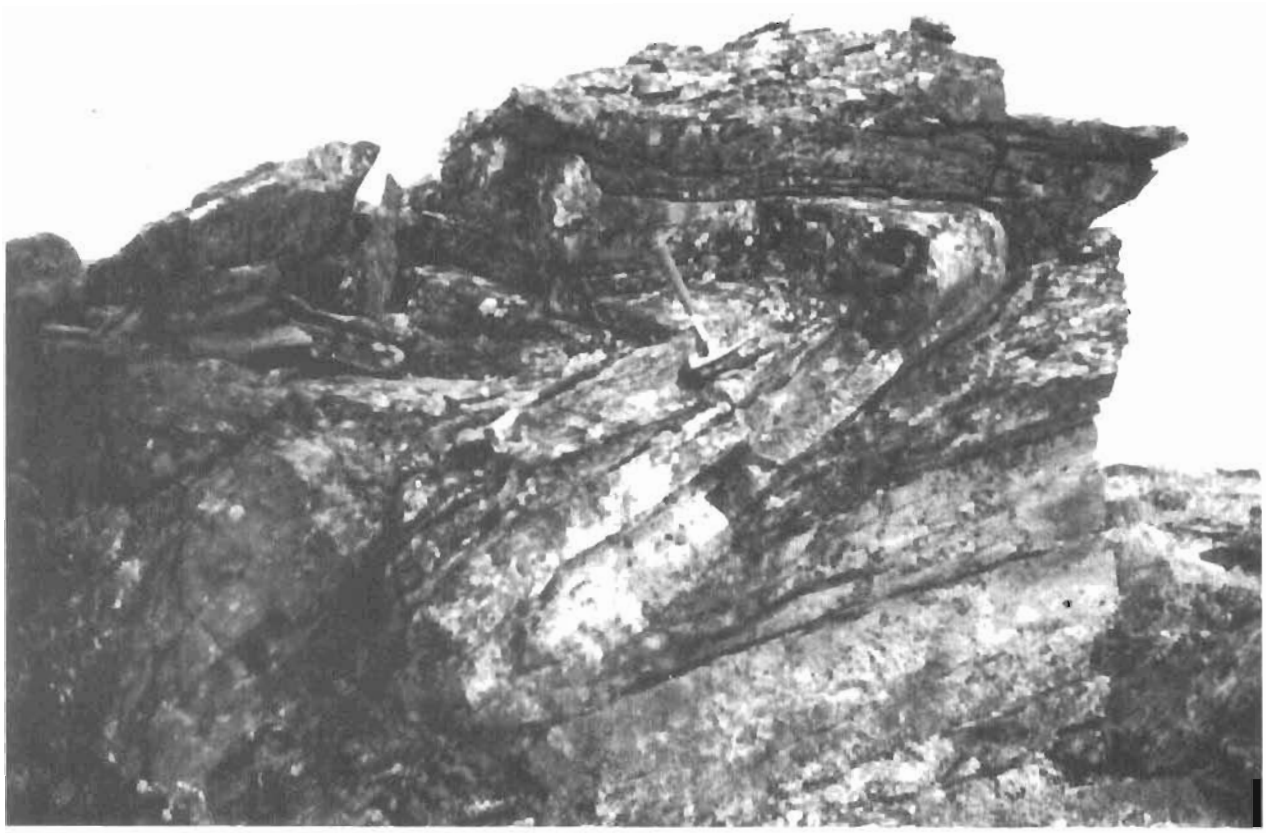

PROFESSIONAL REPORT 86

Published by

DIVISION OF GEOLOGICAL & GEOPHYSICAL SURVEYS

ROSS G. SCHAFF
STATE GEOLOGIST
1984

SHORT NOTES ON ALASKAN GEOLOGY
1982-83

PROFESSIONAL REPORT 86

Recent research on Alaskan geology

STATE OF ALASKA

Bill Sheffield, *Governor*

Esther C. Wunnicke, *Commissioner, Dept. of Natural Resources*

Ross G. Schaff, *State Geologist*

'Short Note' Editorial Policy

This document comprises short contributions on recent investigations of a limited scope on Alaskan geology. Manuscripts are accepted for review with certain qualifications: that manuscripts must not have been published or submitted for publication elsewhere; that all persons listed as authors have given their approval for submission of the paper; and that any person cited as a source of personal communication has approved such a citation.

Two copies of the manuscript, typed double spaced including references and figure captions, should be submitted to Editor, Alaska Division of Geological & Geophysical Surveys, 794 University Avenue, Basement, Fairbanks, AK 99701. No more than seven double-spaced manuscript pages (2000 words), including references, figures, and tables, will be accepted. All figures should be suitable for black-and-white reproduction at a maximum size of 6-1/2 by 8-1/2 inches—foldout or color art will not be accepted. Contributors should keep one copy of material submitted. All manuscripts will be examined and approved by DGGS reviewers. *Substantial changes by the author—whether scientific or editorial—will not be allowed once the manuscript is in galley form.*

Deadline for manuscripts for the next Short Notes on Alaska Geology is September 1, 1985.

Cover photograph: *Isoclinal to subisoclinal fold in metamorphic rocks, Kantishna Hills, Alaska. Photograph by T.K. Bundtzen, 1982.*

DGGS publications are available at: Alaska National Bank of the North Bldg. (2nd floor), Geist Rd. and University Ave., Fairbanks; 3601 C St. (10th floor), Anchorage; 230 So. Franklin St. (4th floor), Juneau; and the State Office Bldg., Ketchikan. Mail orders should be addressed to DGGS, 794 University Ave. (Basement), Fairbanks, AK 99701. Cost $2.50.

CONTENTS

METRIC CONVERSION FACTORS

To convert feet to meters, multiply by 0.3048. To convert inches to centimeters, multiply by 2.54.

AN UNCONFORMITY WITH ASSOCIATED CONGLOMERATIC SEDIMENTS IN THE BERNERS BAY AREA OF SOUTHEAST ALASKA

By Earl Redman[1]

INTRODUCTION

The lack of knowledge of the stratigraphy within and between the lithologic units in the Juneau Gold Belt is a result of both lithologic monotony and the absence of detailed geologic mapping.

Recent mapping for the Hyak Mining Company in the old Jualin Mine area on the north side of Berners Bay, 65 km northwest of Juneau (fig. 1), revealed an angular unconformity within the Berners Bay Group. This feature, herein informally called the 'Jualin unconformity,' marks a period of uplift and erosion some time after intrusion of the Jualin Diorite pluton. The unconformity is overlain by a unit, herein informally named the 'Jualin formation,' that consists of boulder conglomerate, a pebble conglomerate with volcanic detritus, magnetite-bearing conglomeratic sandstone, and metavolcanic rocks that contain fragments of Jualin Diorite.

The apparent truncation of the Jualin gold-quartz veins by this unconformity is economically significant, because post-ore erosion could affect current exploration theories in other parts of the Berners Bay area and the Juneau Gold Belt.

ROCK UNITS OF THE JUALIN AREA

The Jualin area is underlain by the Taku terrane, an apparently upright, southwest-dipping sequence of metavolcanic and metasedimentary rocks of Jurassic to Cretaceous(?) age (Beikman, 1975). Amygdaloidal metabasalt forms the base of the section and is overlain by a sequence of porphyroblastic greenschist, which is overlain by light-colored metasedimentary rocks. The Jualin Diorite intrudes the metabasalt, greenschist, and metasedimentary rocks, all of which are truncated by the Jualin unconformity. This unconformity forms the base of the Jualin formation, a sequence of clastic sedimentary, volcaniclastic, and volcanic rocks.

The basal metabasaltic rocks are not cut by the present trace of the unconformity, but are present as clasts in the posterosion conglomerate. White, spherical amygdules in the metabasalt make it readily identifiable in posterosion conglomerates.

The overlying porphyroblastic greenschist is composed of metamorphosed intermediate and minor felsic volcanic and volcaniclastic rocks: it is dominated by abundant 1-mm-diam porphyroblasts of feldspar. Several thin layers of chlorite and muscovite schist that locally contain thin, concordant beds of abundant or massive sulfides are scattered throughout the unit.

Atop the greenschist is a dense, microcrystalline, gray metasedimentary section that exhibits poor to good slaty cleavage that is generally overprinted by hornfelsing from intrusion of the Jualin Diorite.

The medium-grained Jualin Diorite forms an elongate pluton intruded along the regional grain parallel to the trend of the bedded units of the Jualin area. Magnetite is an abundant accessory mineral. A long arm of the main pluton parallels Snowslide Gulch and concordantly intrudes the metasedimentary unit.

Hornblendite is an unusual coarse-grained rock tentatively correlated with the hornblendite of Knopf (1911). Its stratigraphic position is uncertain, but it is overlain by the erosional conglomerate.

The Jualin formation was deposited on the unconformity and consists of two lithologic packages: a) terrestrial clastic sediments and b) terrestrial to marine volcanic and volcaniclastic rocks. Conglomerates directly overlie the Jualin unconformity and are the most easily traced indicator of it.

Black fissile slate and subordinate graywacke and argillite interfinger with the upper part of the Jualin formation and form the uppermost part of the section of the Taku terrane. The slate includes an isolated section of intermediate and felsic volcanic rocks a few hundred meters above its base.

THE JUALIN UNCONFORMITY

The Jualin unconformity has been traced for 6.5 km from Tangen Creek to the Sherman Creek drainage. Although marked by a string of conglomerate outcrops, the actual unconformity has been seen in only five locations. The three best exposures are shown on figure 2.

The unconformity represents a period of uplift of uncertain duration and magnitude. At least 200 m of the metasedimentary unit has been removed from between the Jualin Mine and Snowslide Gulch. The southern extension of the gold-quartz veins mined at the Jualin Mine disappear near the trace of the erosion surface. On

[1]C.C. Hawley & Associates, Anchorage, Alaska 99507.

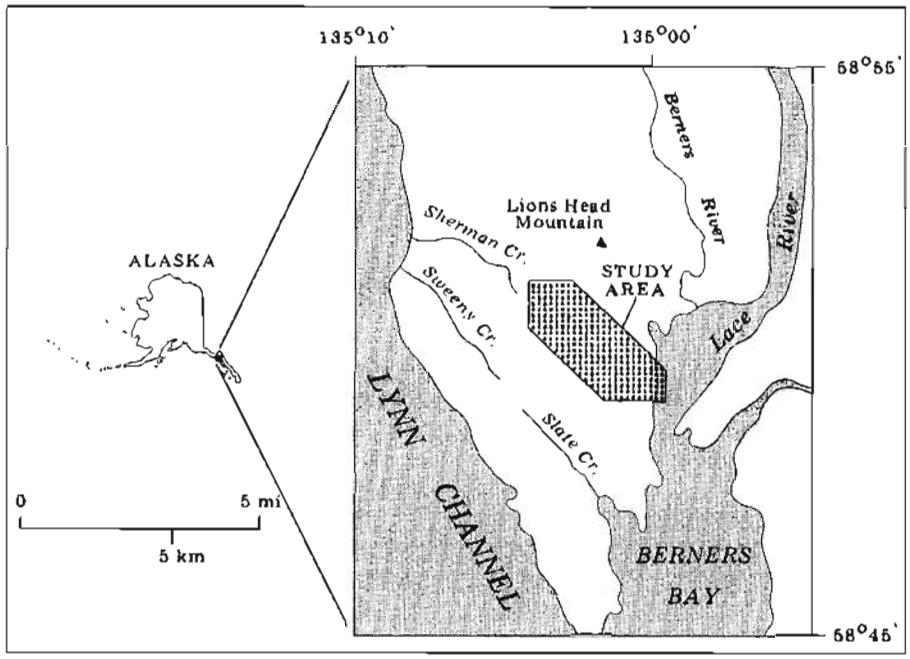

Figure 1. Location of study area.

lower Johnson Creek, north of location 3 (fig. 2), the unconformity may cut the porphyroblastic greenschist.

THE JUALIN FORMATION

The Jualin formation is composed of a clastic member and a volcaniclastic and volcanic member. The former consists of three gradational units: a) boulder conglomerate, b) pebble conglomerate, and c) a magnetite-bearing transition unit.

Boulder Conglomerate

The boulder conglomerate is a local unit that always lies directly on the erosional surface and may represent old stream channels on a terrestrial surface. At location 1 (fig. 2), a boulder-filled channel can be seen in cross section cut into the Jualin Diorite apophysis and overlain by a well-imbricated pebble conglomerate. As elsewhere in the boulder conglomerate, a large percentage of the clasts in the channel are composed of fragments of the underlying bedrock. The most common clasts in the boulder conglomerate are Jualin Diorite, metabasalt, and light-colored metavolcanic rock with a lesser amount of metasedimentary fragments up to 40 cm long. Dark, rounded fragments of metabasalt with distinct white amygdules are conspicuous. The boulder-conglomerate unit may grade upward into or be unconformably overlain by the pebble conglomerate.

Pebble Conglomerate

The pebble conglomerate, about 15 m thick, consists of light-colored metavolcanic and metasedimentary clasts in a sandy matrix. The pebbles are strongly imbricated and are remarkably consistent in size. Clasts are rounded, elongate, about 1 to 2 cm long, and oriented parallel to the unconformity surface. A few fragments of Jualin Diorite and metabasalt are present.

The pebble conglomerate may overlie the boulder conglomerate, lie directly on the unconformity surface (loc. 1, fig. 2), or be separated from the unconformity by a thin tuffaceous layer (loc. 3, fig. 2). At location 3, the conglomerate lies on top of a 1-m-thick tuffaceous bed and contains no fragments of the underlying hornblendite.

The pebble conglomerate grades upward into the magnetite-bearing transition unit. This gradation is characterized by a general decrease in the percentage of pebble-sized clasts.

Magnetite-bearing Transition Unit

Near the uppermost part of the conglomeratic section, magnetite-rich sandstone is very conspicuous. It varies from conglomeratic sandstone to sandstone and is lithologically distinct because it contains up to 80 percent magnetite (loc. 2, fig. 2). The magnetite layers are remarkably well sorted, display cross-bedding, and appear to represent clean fluvial channel deposits. Gold concentrations in the magnetite-rich sandstone are

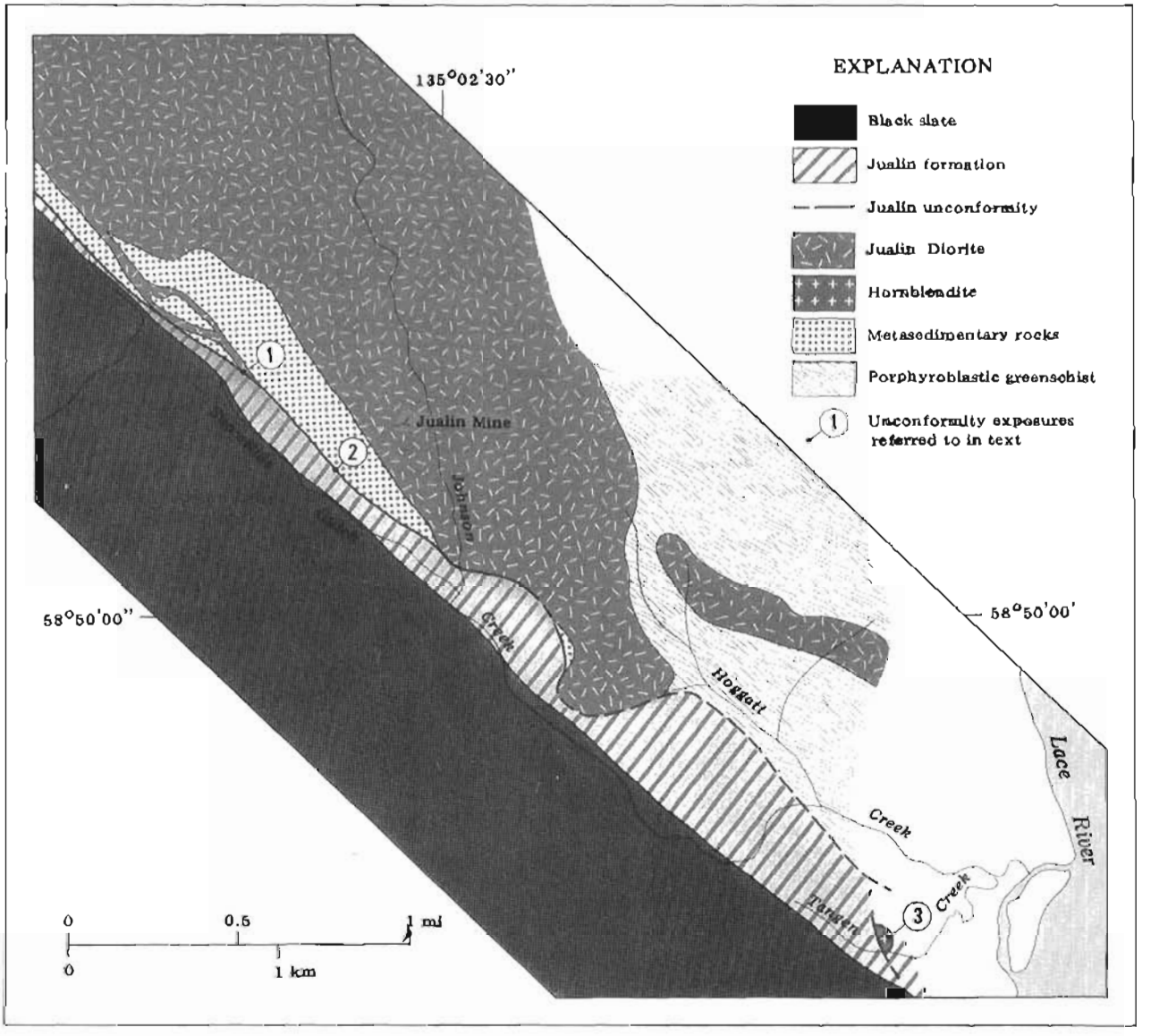

Figure 2 Geology of the Jualin Mine area.

distinctly above background.

The transition unit is about 6 m thick and can be traced for 200 to 300 m northwest from locality 2. The unit grades into the upper volcaniclastic and volcanic unit with increasing tuffaceous sandstone layers.

Volcaniclastic and Volcanic Member

Above the magnetite-bearing transition unit, the rocks grade from tuffaceous sandstone to volcanic flows and volcaniclastic rocks. The metavolcanic rocks, which are predominately green, include felsic and intermediate volcanic flows and volcaniclastic tuffs. This unit also contains a distinct horizon containing thinly interbedded layers of muscovite-chlorite schist with both stratiform-sulfide and massive-sulfide mineralization.

GEOLOGIC HISTORY

Both the unconformity and the overlying clastic sediments probably represent uplift of the Jualin area and subsequent deposition of several hundred meters of eroded material. Fluvial deposition with simultaneous terrestrial volcanic deposition followed the erosional period. The earliest depositional period, represented by the boulder-conglomerate channels, occurred in a high-energy fluvial environment. With reduced stream gradients came contemporaneous deposition of the pebble conglomerate and volcaniclastic detritus. Locally,

the terrestrial volcanic tuffs and flows were deposited before the pebble conglomerate (loc. 3, fig. 2) and provided much detritus for the conglomerates. A welded tuff(?) with fragments of Jualin Diorite also occurs within the pebble-conglomerate section. As stream gradients decreased, the stream-channel sediments became more sandy; with further erosion, the tuffaceous sandy sediments and magnetite (probably derived from erosion of the Jualin Diorite) were concentrated in the stream channel. Continued volcanic activity accompanied by gradual subsidence deposited a sequence of marine volcanic flows and volcaniclastic rocks. The massive-sulfide horizon evinces a marine environment.

SUMMARY

The Jualin unconformity represents a period of uplift and erosion during a time dominated by marine volcanism and sedimentation. The regional extent and significance of the unconformity are not clear, but its local significance is obvious, especially if it removed the upper part of the gold mineralization, as at the Jualin Mine.

If the unconformity is regional, the boulder conglomerate may contain economic quantities of gold in paleoplacer deposits throughout the Berners Bay region. Nevertheless, further geologic mapping is needed to delineate the extent of the Jualin unconformity to determine its importance elsewhere in the Juneau Gold Belt.

ACKNOWLEDGMENTS

I thank Neil MacKinnon of Hyak Mining for permission to present this material and conclusions. I also appreciate the editorial advice of Bill Roberts and Cory Samla (U.S. Bureau of Mines) and the reviews of DGGS geologists W.G. Gilbert and G.H. Pessel.

REFERENCES CITED

Beikman, H.M., 1975, Preliminary geologic map of southeastern Alaska: U.S. Geological Survey Miscellaneous Field Studies Map MF-673, scale 1:1,000,000.

Berg, H.C., Jones, D.L., and Coney, P.J., 1978, Map showing pre-Cenozoic tectonostratigraphic terranes of southeastern Alaska and adjacent areas: U.S. Geological Survey Open-file Report 78-1085, scale 1:1,000,000, 2 sheets.

Knopf, Adolph, 1911, Geology of the Berners Bay region, Alaska: U.S. Geological Survey Bulletin 502, 61 p.

AN IRON-RICH LAVA FLOW FROM THE NENANA COAL FIELD, CENTRAL ALASKA

By S.P. Reidel[1]

INTRODUCTION

The Nenana coal field, located in the northern foothills of the Alaska Range (fig. 1a), is situated in a series of synclinal basins that contain Tertiary coal-bearing rocks (Wahrhaftig and others, 1969). The coal-bearing group consists of five formations: the Healy Creek, Sanctuary, Suntrana, Lignite Creek, and Grubstake Formations. The Nenana coal field has been mapped and described by Wahrhaftig (1970a-h) and Wahrhaftig and others (1969).

This paper describes a previously unreported volcanic unit that is intercalated with nonmarine sediments of the coal-bearing group in the Nenana coal field. The field relationships and preliminary data on chemical composition and mineralogy are the focus of this report.

OCCURRENCE AND DESCRIPTION

The volcanic unit consists of two flows: a) a thin (less than 3-m-thick), dark-gray flow that resembles basalt and b) an underlying rhyolite. The basaltlike rock does not have the typical nonmetallic black appearance of basalt, but is dark gray with a metallic to submetallic luster. Weathered surfaces commonly oxidize red and resemble the oxidized tops of basalt flows.

This lava flow contains many intraflow structures that commonly develop in intermediate and mafic lavas as they cool. Intraflow structures generally present only in flows at least tens of meters thick can be observed in hand specimen. Columnar jointing that includes both colonnades and entablatures (fig. 2) is present in several locations, but the average column diameter rarely exceeds several millimeters. Fanning columns (fig. 3) and columns that formed so rapidly that they separated from each other are especially well developed at site B (fig. 1a).

Typically, the basaltlike flow is poorly exposed, but oxidized surfaces such as those at site A (fig. 1a) are recognizable from the air. The rock is highly magnetic, however, and produces distinct aeromagnetic anomalies where thicker exposures occur at shallow depths (fig. 1b).

The flow was sampled and described at three locations (fig. 1a, sites A-C). The westernmost exposure (site B), on the east side of California Creek in the Rex coal basin, is exposed along the crest of a small east-west-trending ridge that was mapped as the Suntrana Formation by Wahrhaftig (1970g). The underlying sediments have been contact metamorphosed and in places mixed with the lava, which indicates an invasive relationship. The invasive character and the presence of very small intraflow structures in the flow suggest the lava chilled in wet, poorly lithified sediments.

The flow is also exposed along Mystic Creek, in the Mystic coal basin (site C, fig. 1a). The flow is intercalated with a red, contact-metamorphosed siltstone (fig. 4) that was mapped by Wahrhaftig (1970a) as an undifferentiated coal-bearing group. The flow, which is only about 1 cm thick, is poorly exposed here. The lava fills cracks in the siltstone, which is altered less than 1 m both above and below, also indicating the invasive nature of the flow at this locality.

The easternmost site (A, fig. 1a) occurs on the east side of Dry Creek, where the basaltlike flow overlies a rhyolite. The contact between the two is sharp and shows no evidence of a paleosol, which suggests a very short period between eruptions. The rhyolite is about 4 to 5 m thick, is blocky and vesicular with rare microphenocrysts of feldspar, and has a vitreous luster. It has an unusually low density, probably owing to pervasive vesicles. This is the only rhyolite that was observed.

The drainage system during the time of deposition of the Suntrana Formation, based on the probable age of the volcanic unit, was east to west (Wahrhaftig and others, 1969), as indicated by paleocurrent directions in the Tatlanika Creek and Wood River areas. This suggests that the vent area is at or east of site A (fig. 1a). The flow is interpreted to have erupted near Dry Creek and flowed west through the paleodrainage system, finally cooling and solidifying in the structurally controlled coal basins. On the basis of known localities (fig. 1a) and the areal control imposed by the structural basins, the basaltlike flow may have originally covered as much as 1,000 km^2 and, assuming an average thickness of 1 m, its probable volume does not exceed 1 km^3.

CHEMICAL COMPOSITION

Representative chemical compositions for the rhyolite and overlying basaltlike flow are given in table 1. The chemical composition for the rhyolite (SR80-1) is

[1]Department of Geology, Washington State University, Pullman, Washington 99164.

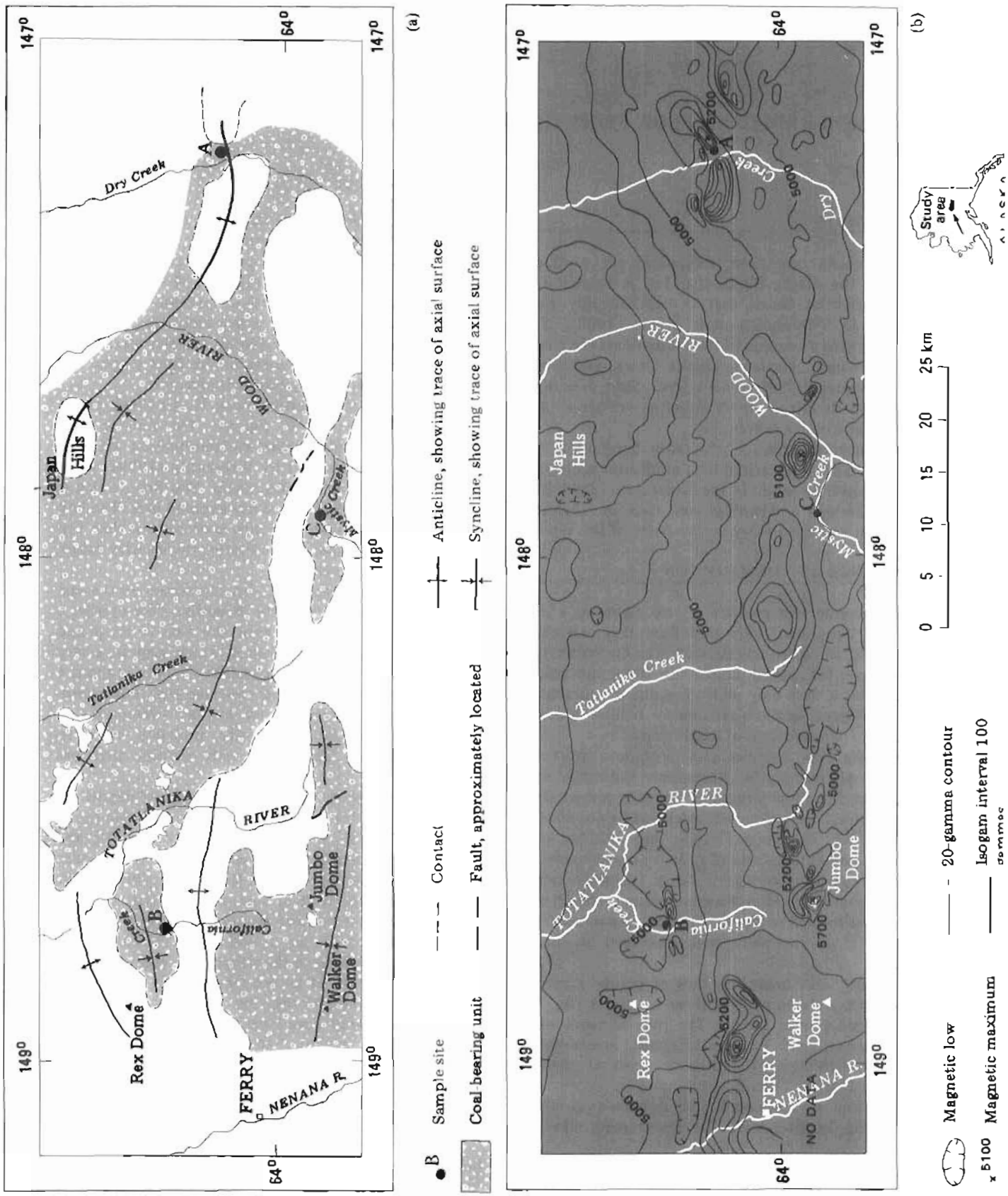
(a)
(b)
147°
148°
149°
64°
Dry Creek
Japan Hills
WOOD RIVER
Tatlanika Creek
TOTATLANIKA RIVER
California Creek
Jumbo Dome
Walker Dome
Rex Dome
FERRY
NENANA R.
McKinley Creek
Sample site
Coal-bearing unit
Contact
Fault, approximately located
Anticline, showing trace of axial surface
Syncline, showing trace of axial surface
Magnetic low
Magnetic maximum
20-gamma contour
Isogam interval 100 gammas
5000
5100
5200
5700
0 5 10 15 20 25 km
Study area

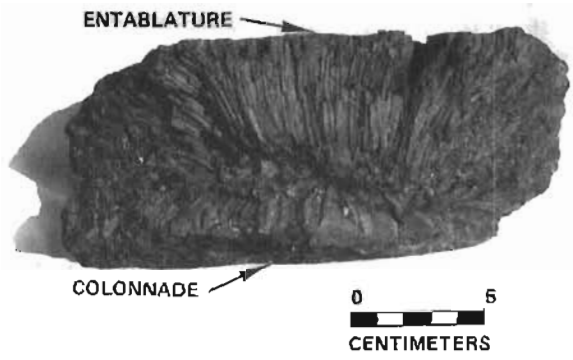

Figure 2. Columnar jointing in the basaltlike lava flow from the Rex coal basin, east side of California Creek (site B, fig. 1a). Small columns are typical of the entablature, and larger columns are analogous to the colonnade.

Table 1. *Representative X-ray fluorescence analyses of samples (in weight-percent).*

Sample	SR80-1	SR80-2
SiO_2	72.50	11.90
Al_2O_3	17.00	4.17
CaO	0.83	0.76
MgO	0.28	0.61
Na_2O	2.12	0.08
K_2O	3.89	0.60
FeO[a]	1.53	73.20
MnO	0.03	0.59
TiO_2	0.30	0.23
P_2O_5	0.06	0.05
LOI[b]	-0.92	0.50
Total	97.62	92.69

[a]Total iron reported as FeO.
[b]Loss on ignition.

typical for rhyolites, but the overlying lava (SR80-2) is dominated by iron, which ranges from 45 to 74 weight-percent, several times that of average basalts (Nockolds, 1954). The SiO_2 content ranges from 12 to 30 weight-percent and Al_2O_3 (4 to 11 weight-percent) is the only other significant oxide. (In two samples analyzed, CaO and MgO approached several weight-percent.)

The chemical composition of the iron-rich lava differs from common igneous rocks and suggests that the mineralogy is probably dominated by an iron-oxide phase, with lesser contributions from a silicate phase.

Figure 1a. Map of the Nenana coal field in the northern foothills of the Alaska Range; generalized from Wahrhaftig (1970a-h).

Figure 1b. Aeromagnetic anomaly map of the area shown in figure 1a; isogam interval is 100 gammas; data from Alaska DGGS (1973a,b).

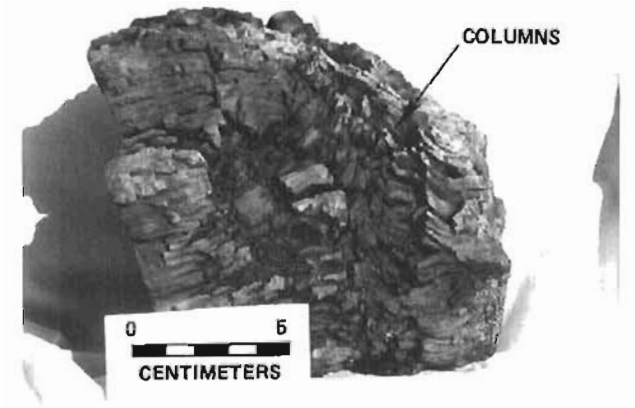

Figure 3. Fanning columnar jointing from site B (fig. 1a). Individual columns that separated from other columns were probably formed by rapid chilling of the lava.

PETROGRAPHY

Preliminary petrographic studies of polished thin sections indicate that at least five phases are present in the iron-rich lava: one glass phase, two silicate-mineral phases, and two opaque phases. The opaque phases dominate the rock and account for the submetallic to metallic luster, whereas the glass phase and the silicate-mineral phases constitute less than 30 volume percent of the rock.

Magnetite has been optically identified, but is almost completely altered to hematite.

Electron-microprobe analyses indicate that the glass is of variable composition, with one end member having the same composition as the rhyolite. The magnetite-hematite phases yield a compatible chemical composi-

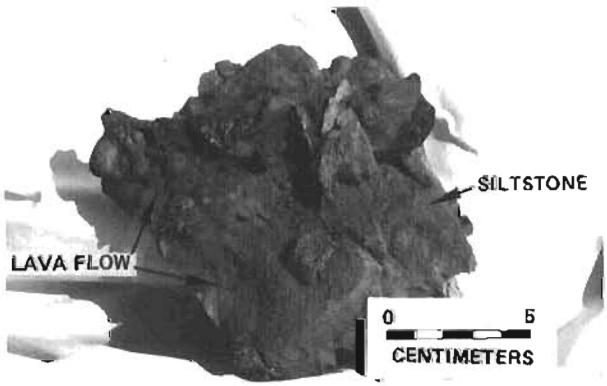

Figure 4. Basaltlike lava that intrudes and covers red baked siltstone from the Mystic Creek coal basin (site C, fig. 1a). The flow intruded layers of sediment and flowed down fractures in the siltstone. The extremely low viscosity is shown by the thinness (less than 1 cm) and wide extent of the flow.

tion, and the silicate minerals have been tentatively identified as fayalite and pyroxene.

CONCLUSIONS

An iron-rich Miocene lava flow observed in the Nenana coal field is equivalent to the Suntrana Formation of Wahrhaftig (1970a-h). The lava was erupted shortly after a low-volume rhyolite and proceeded to flow west through the Miocene drainage system that was controlled by the synclinal coal basins. The low-viscosity lava spread widely.

The composition of the glass suggests that the iron-rich lava flow is a mixture of rhyolite and an iron-rich unit, perhaps a remobilized iron deposit. The rhyolite was probably the transporting medium and assimilated the iron-rich material at depth. Fayalite and pyroxene formed as reaction products.

ACKNOWLEDGMENTS

The thoughtful reviews of J.A. Caggiano, R.D. Merritt (DGGS), and D.N. Solie (DGGS) are greatly appreciated.

REFERENCES CITED

Alaska Division of Geological and Geophysical Surveys, 1973a, Aeromagnetic survey, east Alaska Range, Fairbanks Quadrangle, Alaska: scale 1:250,000, 1 sheet.

Alaska Division of Geological and Geophysical Surveys, 1973b, Aeromagnetic survey, east Alaska Range, Healy Quadrangle, Alaska: scale 1:250,000, 1 sheet.

Nockolds, S.R., 1954, Average chemical composition of some igneous rocks: Geological Society of America Bulletin, v. 65, p. 1007-1032.

Wahrhaftig, Clyde, Wolfe, J.A., Leopold, E.B., and Lanphere, M.A., 1969, The coal-bearing group in the Nenana coal field, Alaska: U.S. Geological Survey Bulletin 1274-D, 30 p.

Wahrhaftig, Clyde, 1970a, Geologic map of the Healy D-2 Quadrangle, Alaska: U.S. Geological Survey Quadrangle Map GQ-804, scale 1:63,360.

_____, 1970b, Geologic map of the Healy D-3 Quadrangle, Alaska: U.S. Geological Survey Quadrangle Map GQ-805, scale 1:63,360.

_____, 1970c, Geologic map of the Healy D-4 Quadrangle, Alaska: U.S. Geological Survey Quadrangle Map GQ-806, scale 1:63,360.

_____, 1970d, Geologic map of the Healy D-5 Quadrangle, Alaska: U.S. Geological Survey Quadrangle Map GQ-807, scale 1:63,360.

_____, 1970e, Geologic map of the Fairbanks A-2 Quadrangle, Alaska: U.S. Geological Survey Quadrangle Map GQ-808, scale 1:63,360.

_____, 1970f, Geologic map of the Fairbanks A-3 Quadrangle, Alaska: U.S. Geological Survey Quadrangle Map GQ-809, scale 1:63,360.

_____, 1970g, Geologic map of the Fairbanks A-4 Quadrangle, Alaska: U.S. Geological Survey Quadrangle Map GQ-810, scale 1:63,360.

_____, 1970h, Geologic map of the Fairbanks A-5 Quadrangle, Alaska: U.S. Geological Survey Quadrangle Map GQ-811, scale 1:63,360.

RESULTS OF A SHALLOW SEISMIC SURVEY FOR GROUND WATER AT McGRATH, ALASKA

By J.F. Meyer,[1] L.L. Dearborn,[2] J.A. Munter,[2] and D.L. Krouskop[1]

INTRODUCTION

In the spring of 1982, the City of McGrath asked the Alaska Division of Geological and Geophysical Surveys (DGGS) to assist them in identifying the potential ground-water supply at Cranberry Ridge, a site proposed for relocation of the present townsite, 4 mi to the northwest (fig. 1).

Potable drinking water has been difficult to obtain in McGrath for many years. Shallow permafrost, low well yields, and ground water with high iron concentration, high dissolved solids, and extreme hardness have resulted in poor well water. In fact, poor water quality caused the U.S. Public Health Service to cap two wells (Kramer, 1979).

On June 16 and 17, 1982, DGGS ran a seismic-refraction survey on Cranberry Ridge to determine whether the Ridge is underlain by permafrost, water-saturated sediments, bedrock, or a combination thereof.

GENERAL GEOLOGIC DESCRIPTION

Cranberry Ridge overlooks the Kuskokwim River from the western edge of a gently rolling terrace of eolian origin (Fernald, 1960). Dunelike topography extends from the Ridge to the south and east, and river bluffs about 100 ft high separate the Ridge from the Kuskokwim River flood plain on the north and west. Old meander scars, some containing boggy oxbow ponds, are present at the base of the bluffs.

A deep cut for a road from McGrath to Cranberry Ridge exposes about 50 ft of medium- to well-sorted, very fine to medium-grained uncemented eolian sand. The total thickness of these sediments is unknown. The only deep well on record (fig. 1) was drilled at the present townsite of McGrath by the Civil Aeronautics Authority in 1948. The well log indicates a depth to bedrock (reportedly slate) of 230 ft.

DATA ACQUISITION AND REDUCTION

Two reversed seismic lines were shot near the top of Cranberry Ridge with a 12-channel Geometrics Nimbus ES-120 signal-enhancement seismograph. Line 1 was shot along Cranberry Ridge Road, and line 2 was shot in a north-south direction almost perpendicular to and intersecting line 1 (fig. 2). The geophone interval was 10 ft for the first 240 ft, followed by 20-ft intervals to the maximum offset of 1,100 ft.

The seismic energy was recorded digitally and displayed on paper records for later interpretation. The sample rate for the records was 0.1 ms for the inner geophones and 0.2 ms for the outer geophones. The records were made with a fixed-gain set to allow for maximum relief of the first breaks.

The seismic-energy source consisted of from 1 to 12 blasting caps, depending on the offset, buried in a 2-ft-deep hole. Throughout the survey, the caps made good contact with the ground and caused no surface cratering. The geophones were seated in moist topsoil when possible and in frozen soil when necessary. Rods were used to probe the frozen layer, which was erratically distributed at depths of a few inches to about 1 ft.

First breaks were picked for all the records and were corrected for an instrument-recording delay that was measured by a geophone adjacent to the shot hole. A time-correction factor was also applied to the data to account for differences in elevation between the shot point and the geophones. Surveyed elevations of the geophones were used to correct the arrival times to a seismic datum of 410 ft using the method outlined in Dobrin (1976). Corrected arrival times for each survey line (figs. 3 and 4) were used to plot velocity cross sections using a dipping two-layer model (Dobrin, 1976).

RESULTS

The simple two-layer model constructed for Cranberry Ridge consists of a layer with a compressional velocity of 1,800 ft/sec underlain by a layer with a compressional velocity of 5,400 ft/sec. These velocities are similar to those obtained by Barnes (1965) for a layer of dry, loosely consolidated alluvium underlain by water-saturated alluvium.

On the basis of the quality of the seismic records, the maximum depth of interpretable seismic penetration is about 200 ft below land surface. The lack of higher velocity layers within this depth range indicates that bedrock, which probably has a compressional velocity exceeding 8,000 ft/sec, is not present within about 200 ft of the surface. The near-surface layer of seasonally frozen ground posed no problems in interpreting the seismic records; it was usually penetrated by holes punched for the shots and geophones.

Depths of the inferred water-saturated layer below seismic datum were calculated using a standard dipping

[1]DGGS, Pouch 7-028, Anchorage, Alaska 99510.
[2]DGGS, P.O. Box 772116, Eagle River, Alaska 99577.

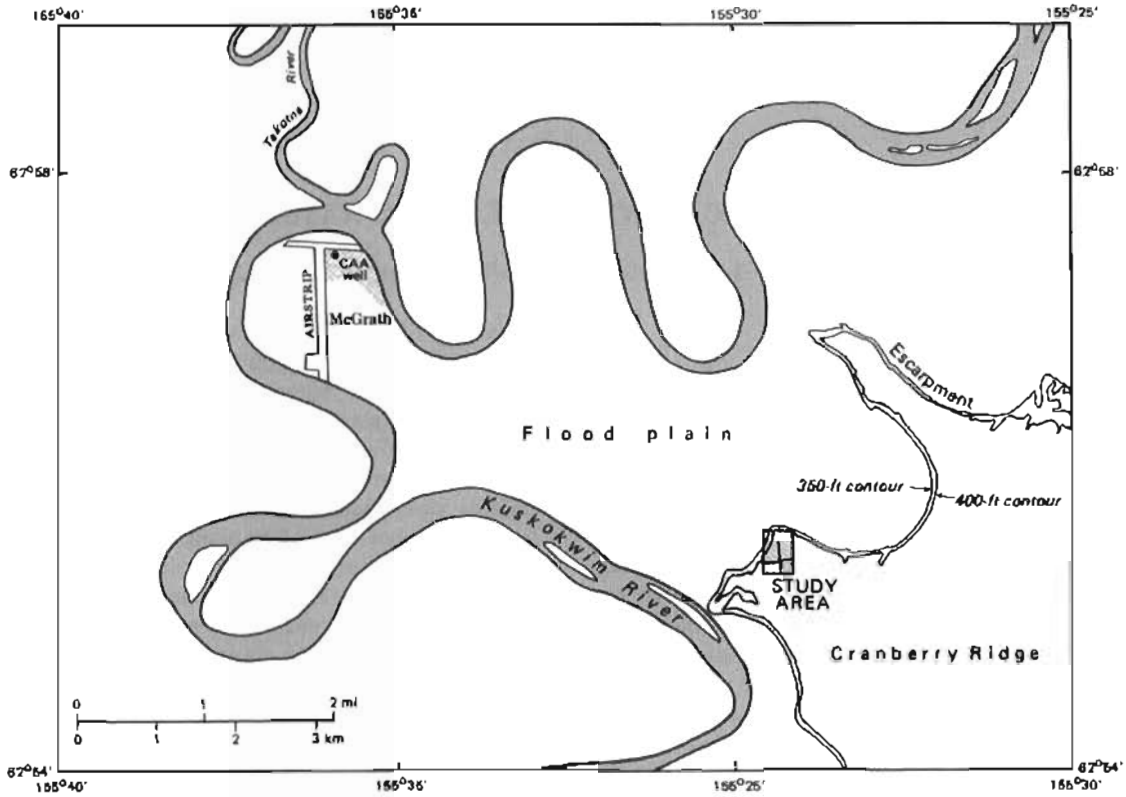

Figure 1. Location of study area (base from U.S. Geological Survey McGrath Quadrangle, Alaska, 1979).

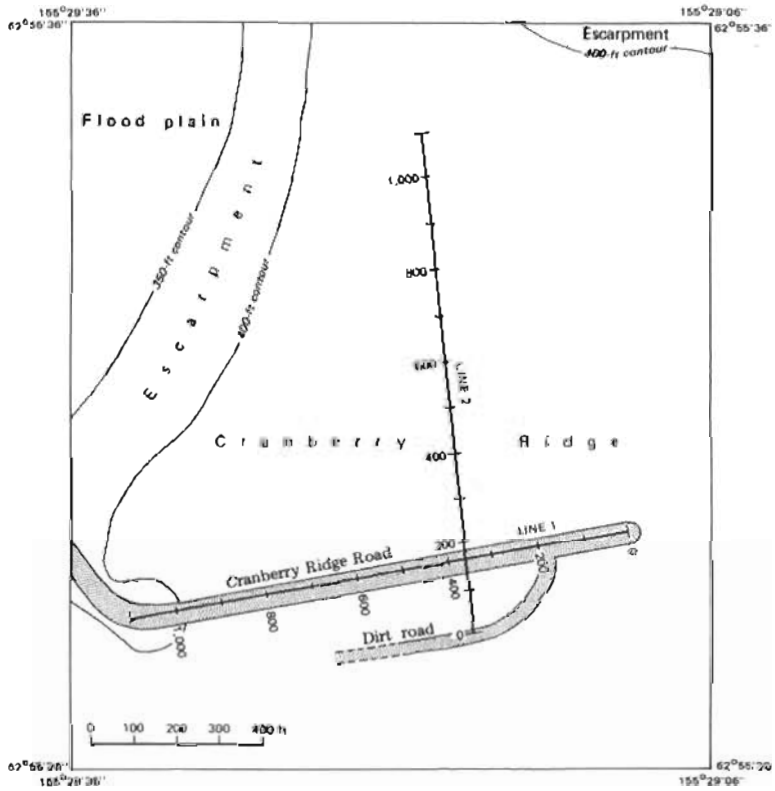

Figure 2. Enlargement of study area showing location of seismic lines.

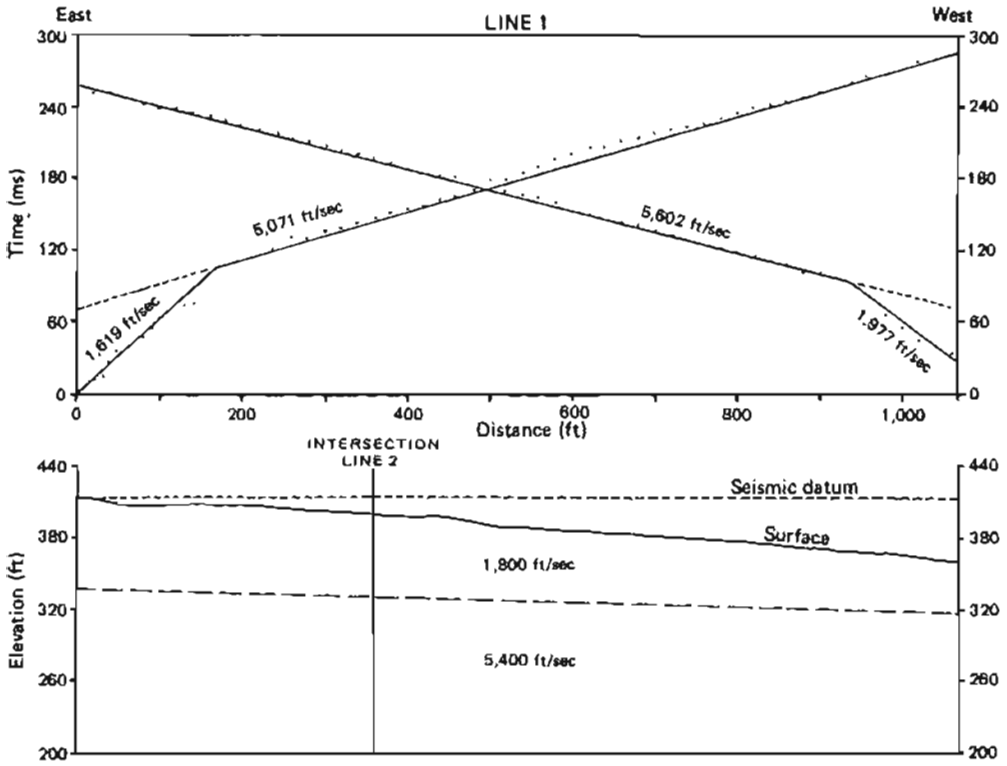

Figure 3. Time-distance curves and velocity section for seismic line 1.

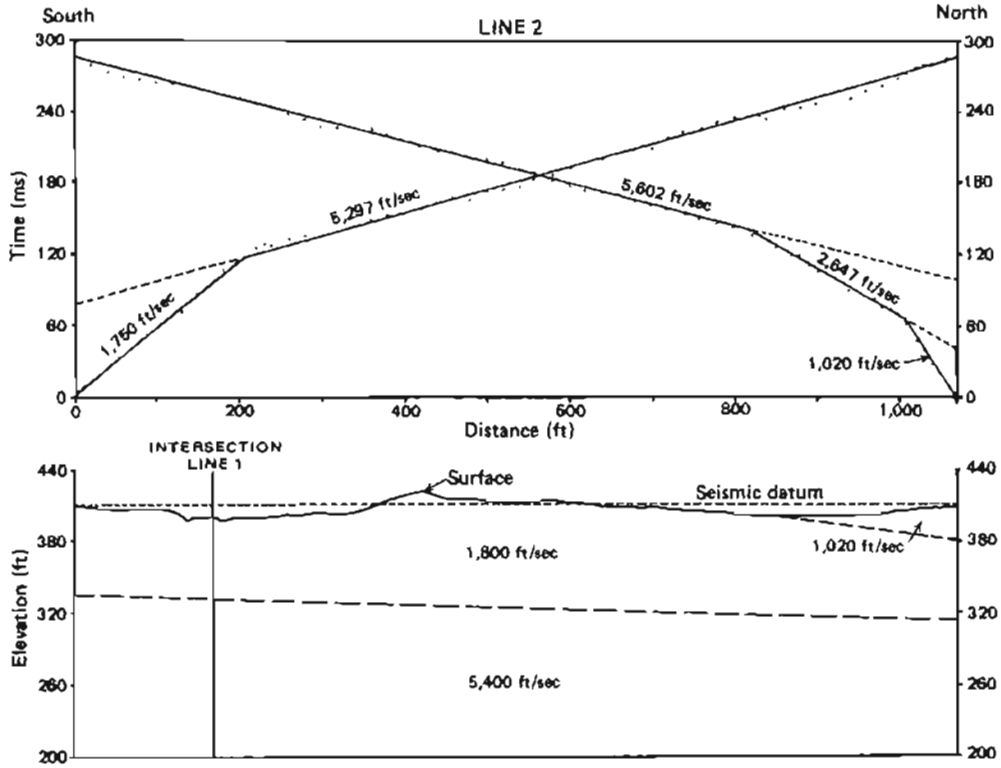

Figure 4. Time-distance curves and velocity section for seismic line 2.

two-layer model (table 1). The dip of the water table, as calculated from the slopes of the interfaces, is northwesterly. This direction of ground-water movement is reasonable because likely recharge sources occur to the southeast. Also, some standing water at the base of the bluff was surveyed at 88 ft below the seismic datum, which also fits well within the depth range calculated for the water-saturated sediments.

Table 1. *Depth of water-saturated layer below seismic datum.*

Seismic profile		Depth
Line	End	(ft)
1	East	72
1	West	92
2	North	97
2	South	74

Drilled wells may provide a solution to the water-supply problem at the new townsite because of the absence of permafrost and the inferred presence of at least 100 ft of saturated sediments. However, silty flood-plain deposits may dominate the section under the water table; if so, the most permeable stratum may support only low-yielding wells. On the other hand, if the sand dunes are older than the geologically recent flood-plain deposits, saturated dune sand should serve as a moderate-yielding aquifer.

ACKNOWLEDGMENTS

This study was funded by the DGGS/U.S. Geological Survey Alaska Water Resources Evaluation (AWARE) program. We enjoyed the cooperation and assistance of Bob Juettner, Gary Ricketts, and Duanne Norbeck of McGrath. We also thank S.T. Cutler and J.T. Kline for reviewing the manuscript.

POSTSCRIPT

During March and April 1983, a water well was drilled for the City of McGrath approximately 300 ft north of the south end of line 2 and 200 ft west of the east end of line 1 (fig. 2). The 6-in.-diam cased hole, drilled with a cable-tool rig, penetrated to a depth of 115 ft below land surface (table 2). The following information was provided by the driller.

Table 2. *Driller's log of Cranberry Ridge water well.*

Depth (ft)	Description of materials
0 - 0.5	Tundra
0.5 - 7	Silty sand (seasonally frozen)
7 - 101	Silty sand (thawed, dry)
101 - 104	Clay, with some vegetation
104 - 115	Sand with some small gravel; screened 110-115 ft

On April 1, 1983, with the open-ended casing at a depth of 107 ft, the driller recorded "28 ft of water static in the pipe." This translates to a water-level depth of 79 ft below land surface, or 324-ft seismic-datum elevation. We believe this water level closely reflects the position of the water table at the site. From the seismic-velocity sections (figs. 3 and 4), the depth to saturation at the well site is projected to be 78 ft. Thus we conclude that the seismic-refraction technique produced results in excellent agreement with the results obtained from subsequent drilling.

REFERENCES CITED

Barnes, D.F., 1965, Geophysical methods for delineating permafrost, *in* International Conference on Permafrost, Lafayette, Ind., 1963, Proceedings: Washington, National Academy of Sciences, National Research Council Publication 1287, p. 349-355.

Dobrin, M.B., 1976, Introduction to geophysical prospecting: New York, McGraw-Hill, p. 292-338.

Fernald, A.T., 1960, Geomorphology of the upper Kuskokwim region, Alaska: U.S. Geological Survey Bulletin 1071-G, p. 191-279.

Kramer, V.J., 1979, Water well analyses, sanitation facilities construction, McGrath, Alaska: U.S. Department of Health and Human Services, Public Health Service, project AN 77-169 unpublished report, 9 p.

EVALUATION OF A SHALLOW SAND-AND-GRAVEL AQUIFER AT EAGLE RIVER, ALASKA

By J.A. Munter[1] and L.L. Dearborn[1]

INTRODUCTION

Domestic and community water systems in Eagle River, Alaska, rely totally on local ground water. Because of the limited extent of productive aquifers in the area (Zenone and others, 1974), only nine wells reportedly capable of yielding more than 100 gallons per minute (gpm) had been drilled in the area prior to 1978 (Johnson, 1979). Thus, the development of a private well reportedly capable of producing 550 gpm was of considerable interest to the Municipality of Anchorage as a potential water-supply source for Eagle River. The aquifer test described here was conducted to obtain information about the hydraulic characteristics and boundary conditions of the aquifer tapped by the private well.

PHYSICAL SETTING

Two wells were used for the aquifer test. The north (production) well, located about 100 ft east of the Glenn Highway and 1.2 mi north of the Glenn Highway bridge across the Eagle River (fig. 1), was constructed with 10-in.-diam casing to a depth of 34.6 ft; 15.3 ft of 10-in.-diam, 250-slot stainless-steel screen extend from the bottom of the casing to the bottom of the well. The south (observation) well is 63 ft from the production well and is of similar construction, except that 6-in.-diam casing and screen were used.

Surficial deposits in the area are part of a large alluvial-fan deposit that consists of "gravel and sand with cobbles and small boulders common" (Schmoll and others, 1971). The land surface slopes gently to the west, except for a hill—mapped as a kame by Schmoll and others (1971)—located 300 ft east of the well development. Surficial deposits are associated with the late Naptowne glaciation, which is late Wisconsinan in age (Reger and Updike, 1983).

An 8-in.-diam hollow-stem auger and a 3-1/4-in.-ID split-spoon sampler were used to drill and core the test hole (TH-1), which is located 33 ft northwest of the production well (fig. 1). An abbreviated geologic log of TH-1 is shown in table 1, and the results of grain-size analyses of eight sample intervals are presented in figure 2. Drilling showed a prepumping saturated thickness of 51 ft for the aquifer.

[1]DGGS, P.O. Box 772116, Eagle River, Alaska 99577.

TEST RESULTS AND INTERPRETATION

The observation well was monitored with a continuous water-level recorder for 3.7 days before the start of the test. The recorder showed that water levels in the aquifer were rising at an average rate of 0.12 ft/day, probably because of seasonal recharge.

The pump in the production well was turned on at 9:30 a.m. on June 11, 1982. The well was pumped continuously for 58.5 hr at a time-weighted average rate of 474 gpm. During the test, the flow rate, measured with an in-line, turbine-style flow meter, fluctuated between 461 and 487 gpm. The pump was shut off before the scheduled end of the test (72 hr) when the water level in the production well neared the intake elevation of the test pump.

Drawdown data recorded in the 6-in.-diam observation well during the test are plotted in figure 3. A correction factor of 0.12 ft/day was applied to the data to compensate for the rising water levels observed prior to the test. The standard Theis (1935) curve was fitted to the data collected during the first 3 min of the test and superimposed on the data plot. Calculations based on this curve match yield a transmissivity value (T) of 1.1×10^5 ft^2/day and a storativity value (S) of 2.2×10^{-2} (fig. 3).

Because Theis's (1935) solution is not perfectly suited to known site conditions, a computer model (Neuman, 1974) was used to assess the influence of delayed gravity response, aquifer anisotropy, and partial penetration of the production and observation wells in the aquifer. Using $T = 1.1 \times 10^5$ ft^2/day, $S = 2.2 \times 10^{-2}$, a specific yield of 0.2, and the site geometry described above, the ratio of horizontal to vertical hydraulic conductivity (K_Y/K_Z) was adjusted until a reasonable fit with the observation-well data was obtained. The early-time drawdown data ($t < 3$ min) fit reasonably well with a model-generated curve using a value of $K_Y/K_Z = 7$, whereas the intermediate- and late-time drawdown data ($t > 4$ min) do not. Because the intermediate-time drawdown data (4 min $< t <$ 300 min) do not show the characteristic leveling off typical of water-table aquifers that undergo delayed gravity response (for example, see Neuman, 1975), and because late-time drawdown data ($t > 300$ min) show a significantly greater rate of decline than could be simulated with the model, substantial variations in model parameters did not yield a drawdown curve that approximated the data.

Partial penetration did not affect these results significantly. We conclude that the most reasonable explanation for the shape of the drawdown curve in figure 3 is that one or more relatively impermeable aquifer boundaries are present near the production well.

The location of aquifer boundaries may be related to the hill 300 ft east of the well field (fig. 1). Surficial exposures on the west side of the hill and 5- to 6-ft-deep excavations at the two highest points of the hill reveal only silty diamicton; no glaciofluvial deposits were encountered. Schmoll (oral commun., 1982), identified this landform as a kame on the basis of aerial-photo-

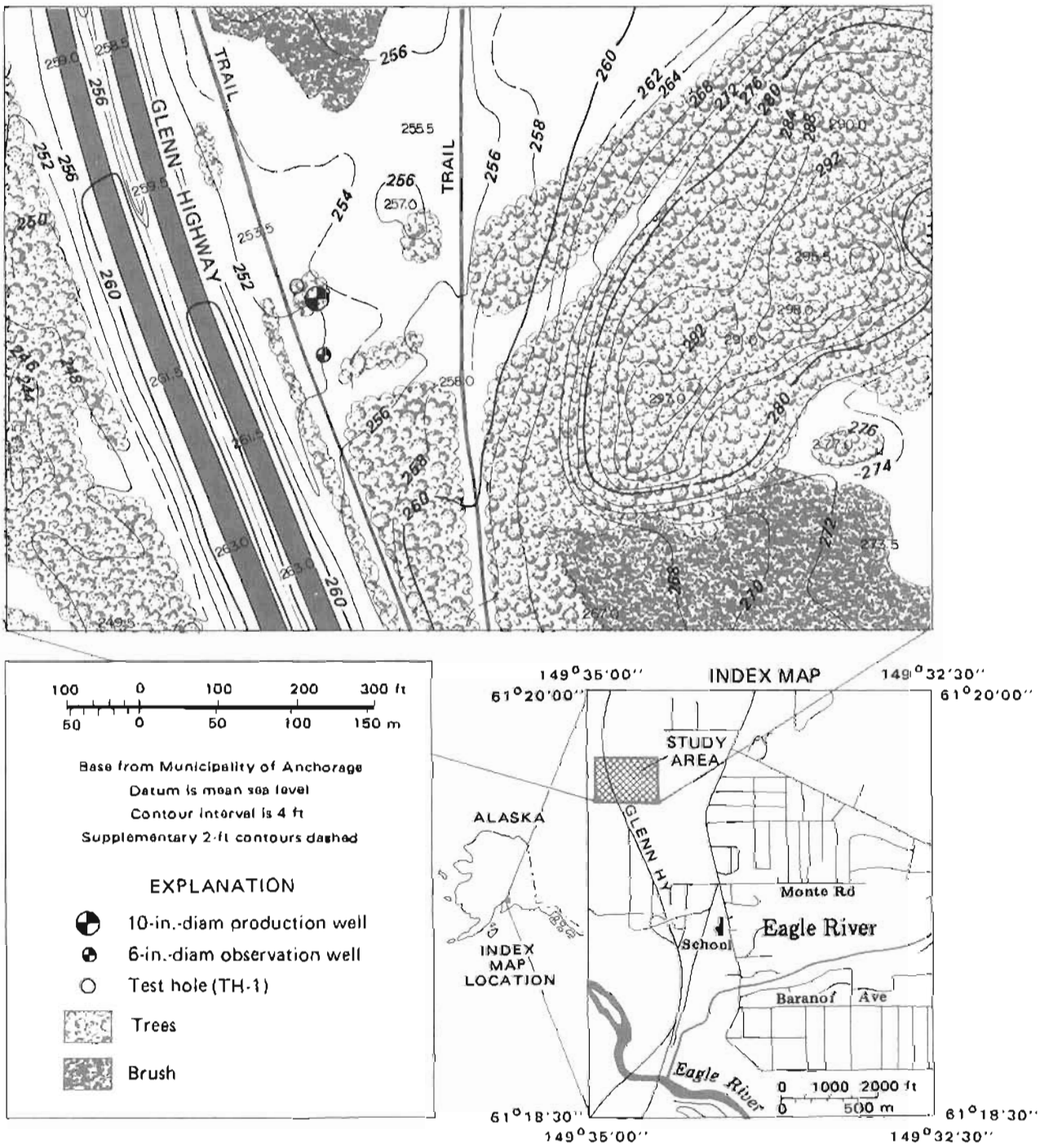

Figure 1. Location of study area, Eagle River, Alaska.

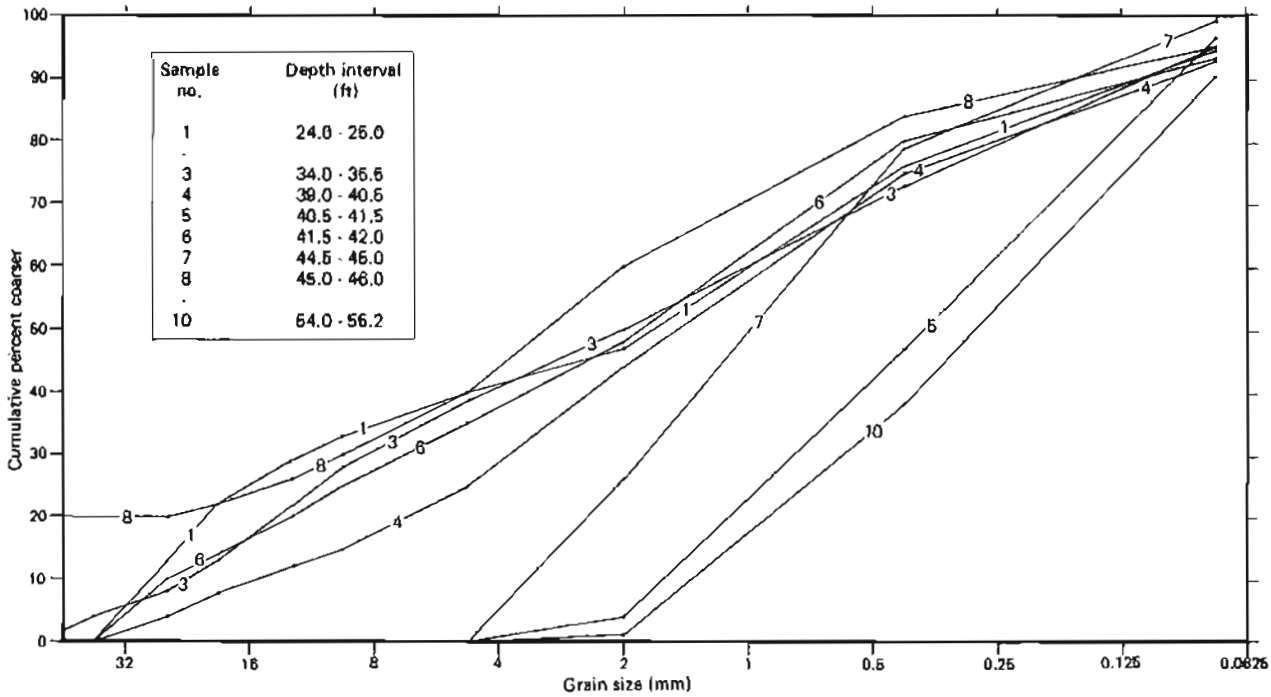

Figure 2. Grain-size analyses of eight sample intervals from test hole (TH-1).

Table 1. *Abbreviated geologic log of test hole (TH-1).*

Depth interval (ft)	Description
0 - 2	Brown silt, organic near top.
2 - 69.5[a]	Brown to gray, interbedded, cobbly, gravelly sand, sandy gravel, and sand; sand dominantly medium- to very coarse grained. Pebbles mostly subrounded to rounded (fig. 2).
69.5 - 70	Light-gray, well-cemented claystone of Kenai Group (Tertiary).

[a]Static water level 17.0 ft below land surface, August 18, 1982.

graph interpretation, not on field examination. From field observations, we reclassify the hill as an erosional remnant of till (probably an outlier of the Elmendorf moraine) that predates the alluvial-fan deposit that surrounds it. Thus, the aquifer is probably truncated 300 ft (or less) to the east of the 10-in.-diam production well.

The drawdown data collected at the production well (fig. 4) were analyzed by a semilog method (Cooper and Jacob, 1946). Transmissivity (8.4 x 10^4 ft^2/day) was calculated using data collected during the first 5 min of pumping. Subsequent data plotted along a curve with a progressively steeper slope and are consistent with data from the observation well, which supports the interpretation that nearby aquifer boundaries influenced the intermediate- and late-time drawdown data.

Water-level data collected at the observation well during the first 7 min of well recovery were matched with a Theis curve to yield a transmissivity of 1.1 x 10^5 ft^2/day and a storativity value of 0.26. The latter value is not reliable because storativity values calculated from early-time data are representative of confined aquifers that typically have values much lower than 0.26.

Recovery data from the production well were also analyzed by the semilog method, and a transmissivity value of 2.0 x 10^4 ft^2/day was obtained. The reason for this relatively low T value is not readily apparent, and reasonable agreement among the other three transmissivity values casts doubt on its validity.

On the basis of transmissivities calculated from the observation-well drawdown and recovery data and from the production-well drawdown data, a transmissivity value of 1.0 x 10^5 ft^2/day is estimated for the aquifer near the well field. This estimate, divided by the prepumping saturated-aquifer thickness of 51 ft, yields an average horizontal hydraulic conductivity of 2.0 x 10^3 ft/day.

The values of transmissivity and hydraulic conductivity calculated from the aquifer-test data are fairly high for aquifers of this type. Specific-capacity values of the well, however, are 320, 210, and 130 gpm/ft of drawdown, based on pumping durations of 10, 100, and 720 min, respectively. Such values of specific capacity

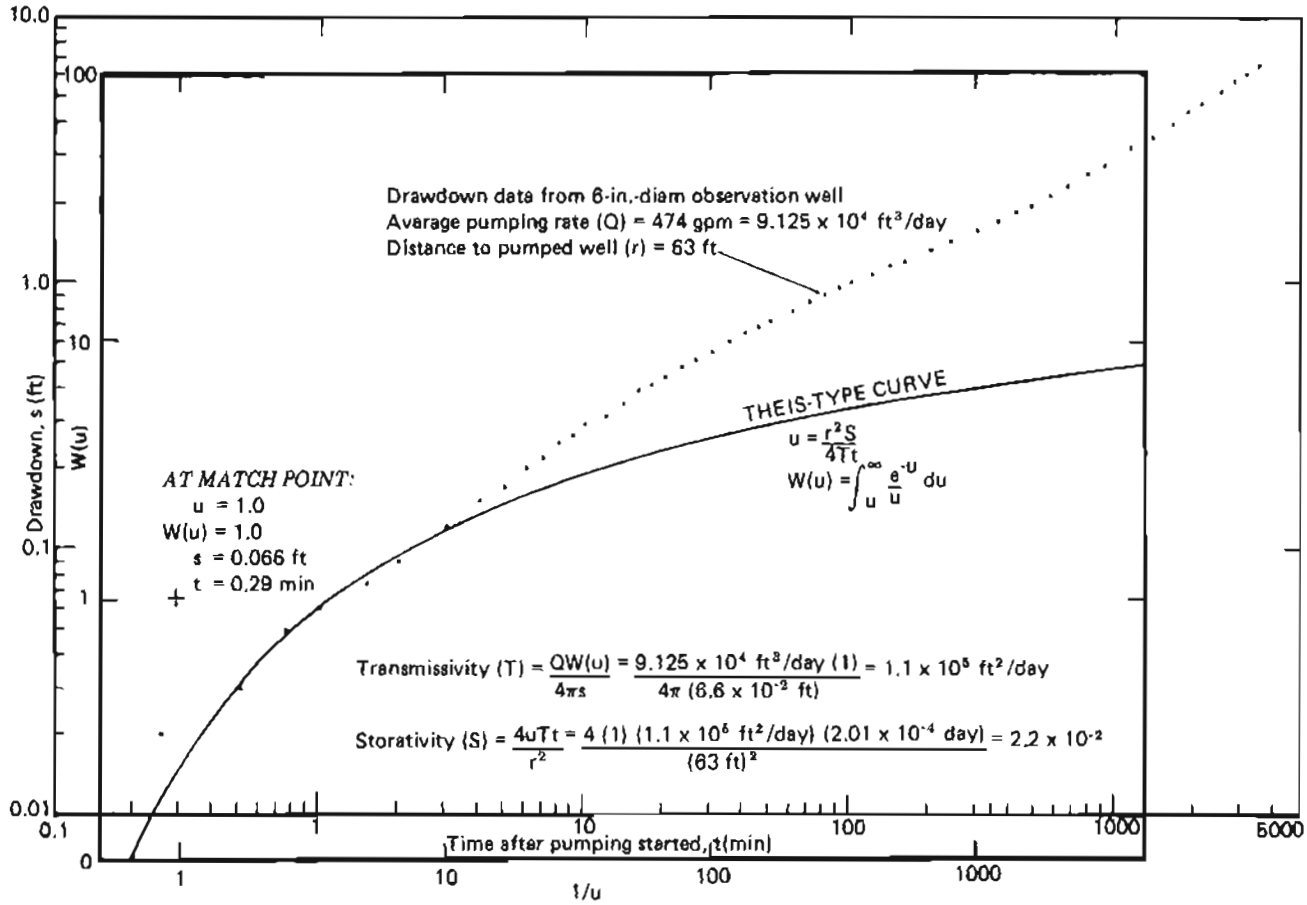

Figure 3. Plot of drawdown data from the 6-in.-diam observation well. Theis curve is superimposed.

are generally indicative of high aquifer transmissivities. Also, the hydraulic conductivity value of 2.0 x 10^3 ft/day is within the range of reported laboratory permeabilities for gravel and is only slightly higher than laboratory values for coarse sand (Morris and Johnson, 1967). Freeze and Cherry (1979, p. 29) suggest that 2 x 10^3 ft/day is near the upper end of the range of values of hydraulic conductivity for clean sand and near the lower end of the range for gravel. In light of these considerations, the field-determined values of transmissivity and hydraulic conductivity are considered reasonable.

As noted, the aquifer water levels were rising at about 0.12 ft/day before the pumping test. Five days after pumping ceased, the rate of water-level rise had decreased to 0.096 ft/day. Full recovery did not occur; the water level in the observation well was 2.5 ft lower than it was at the start of the test. This indicates that the aquifer was stressed beyond its capacity to recover to its prepumping state in a normal manner. The slow addition of water from seasonal recharge, either from the land surface or from up-gradient ground-water influx, appears necessary for full water-level recovery. This coincides with conclusions drawn from drawdown data and reinforces the presence of relatively impermeable aquifer boundaries near the production well.

Laboratory permeability analyses performed on four split-spoon samples (samples 2, 5, 9, 10) of aquifer material are shown in table 2, as are hydraulic conductivity (K) values for three samples (samples 5, 7, 10) from the grain-size data in figure 2. Permeability analyses were performed on samples from two intervals for which Masch and Denny's (1966) method was also used. The five remaining sample intervals were too coarse-grained for analysis by that method.

The hydraulic-conductivity value estimated from the pumping test, 2.0 x 10^3 ft/day, is 700 to 6,000 times greater than the laboratory-measured K values and 90 to 120 times greater than those estimated from the grain-size data. The disagreement between the values is due to the following sampling and analytical limitations:

1. The disruption of bedding and original grain

Table 2. *Sample intervals and laboratory hydraulic conductivity (K) results from test hole (TH-1).*

Sample no.	Sample depth interval (ft)	K value (ft/day) (from permeameter[a])	K value (ft/day) (from grain-size distribution[b])
1	24.0 - 25.0	-	-
2	30.0 - 32.0	0.58	-
3	34.0 - 35.5	-	-
4	39.0 - 40.5	-	-
5	40.5 - 41.5	2.8	16
6	41.5 - 42.0	-	-
7	44.5 - 45.0	-	22
8	45.0 - 46.0	-	-
9	49.0 - 50.0	0.33	-
10	54.0 - 55.2	0.52	17

[a]Method from Lambe (1951). Falling-head method with 2.08 x 10^3 ft^3 permeameter. Material consisted of 100 percent passing 2 mm sieve.
[b]Based on method of Masch and Denny (1966).

fabric and the degree of compaction caused by sampling and repacking the sample in the permeameter.

2. The limited size of the sample and the permeameter compared to the grain-size range of the aquifer.
3. The possibility that sample intervals may not be representative of the dominant aquifer material.
4. A vertically oriented sample was tested in the laboratory, whereas horizontal hydraulic conductivity was calculated from the field data.

Because of these limitations, the values of hydraulic conductivity based on the laboratory data are not considered representative of the hydraulic conductivity of the aquifer near the well field. The discordance between field and laboratory data is notable, however, because in many hydrogeologic investigations the only

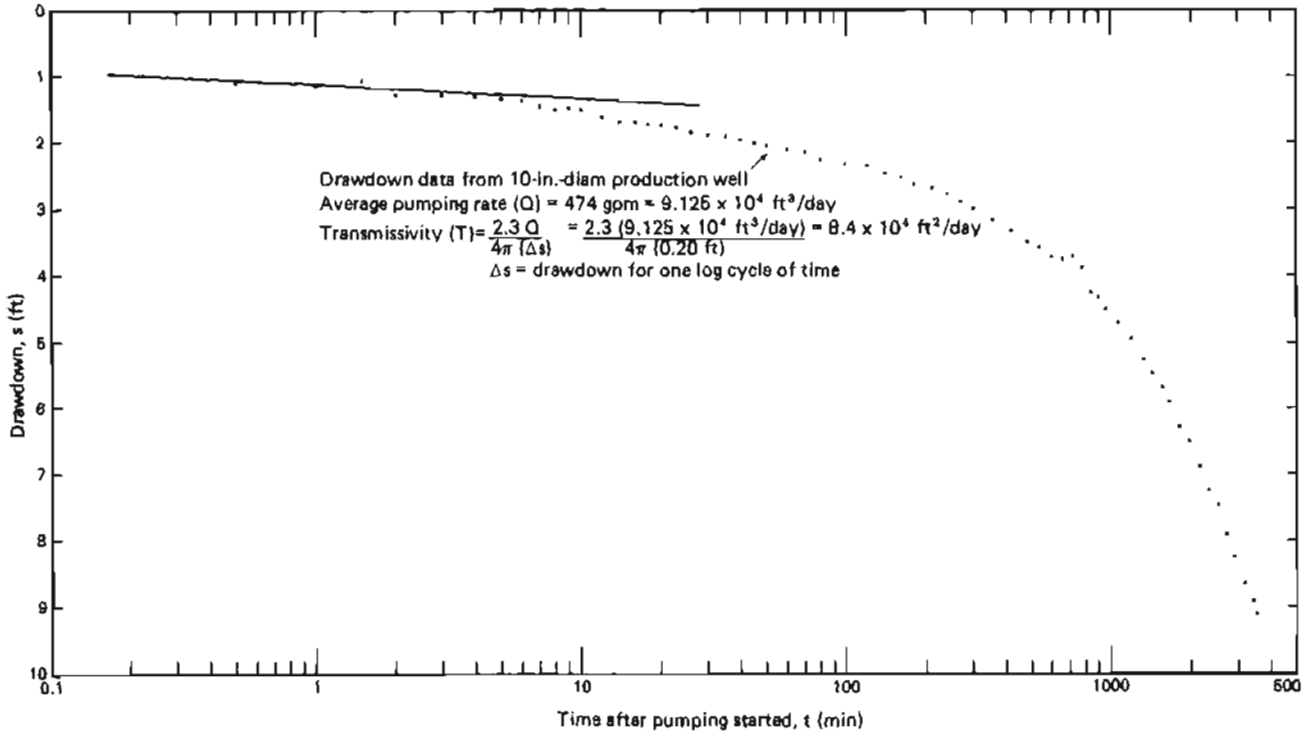

Figure 4. Plot of drawdown data from the 10-in.-diam production well. Straight line used to compute transmissivity.

values of hydraulic conductivity available are obtained from the laboratory.

SUMMARY AND CONCLUSIONS

Interpretation of the aquifer pumping test indicates that the aquifer is highly permeable, but of very limited areal extent. This characterization is supported by the drawdown data obtained from the production well, by the drawdown and early-recovery data at the observation well, and by 5 days of recovery data that show slow and incomplete water-level recovery. Standard laboratory methods of determining hydraulic conductivity yielded values that were anomalously low.

Our investigation suggests that the production potential of the aquifer is strongly influenced by the short-term rate of natural recharge of the aquifer. Thus, although the 10-in.-diam production well initially produced 550 gpm, continued pumping at this rate is not feasible because an excessive decline in water level would occur.

ACKNOWLEDGMENTS

This work was performed in cooperation with the U.S. Geological Survey and the Municipality of Anchorage. We appreciate the logistical support of Quadra Engineering and Anchorage Well and Pump Service. Laboratory analyses were performed by R & M Consultants. The computer code was provided by S.P. Neuman. Although they may not agree with all of our interpretations, special appreciation goes to G.L. Nelson and J.B. Weeks of the U.S. Geological Survey and R.G. Updike of DGGS for helpful reviews of the manuscript.

REFERENCES CITED

Cooper, H.H., and Jacob, C.E., 1946, A generalized graphical method for evaluating formational constants and summarizing well field history: American Geophysical Union Transactions, v. 27, p. 526-634.

Freeze, R.A., and Cherry, J.A., 1979, Groundwater: Englewood Cliffs, New Jersey, Prentice-Hall, 604 p.

Johnson, P., 1979, Hydrogeologic data for the Eagle River-Chugiak area, Alaska: U.S. Geological Survey Water Resources Investigations 79-59, 17 p.

Lambe, W.T., 1951, Soil testing for engineers: New York, Wiley and Sons, p. 52-62.

Masch, F.D., and Denny, K.J., 1966, Grain size distribution and its effect on the permeability of unconsolidated sands: Water Resources Research, v. 2, no. 4, p. 665-677.

Morris, D.A., and Johnson, A.I., 1967, Summary of hydrologic and physical properties of rock and soil materials, as analyzed by the hydrologic laboratory of the U.S. Geological Survey, 1948-1960: U.S. Geological Survey Water-Supply Paper 1839-D, 42 p.

Neuman, S.P., 1974, Effect of partial penetration on flow in unconfined aquifers considering delayed gravity response: Water Resources Research, v. 10, no. 2, p. 303-312.

_____, 1975, Analysis of pumping test data from anisotropic unconfined aquifers considering delayed gravity response: Water Resources Research, v. 11, no. 2, p. 329-342.

Reger, R.D., and Updike, R.G., 1983, Upper Cook Inlet area and Matanuska Valley, *in* Péwé, T.L., and Reger, R.D., eds., Guidebook to permafrost and Quaternary geology along the Richardson and Glenn Highways between Fairbanks and Anchorage, Alaska: Alaska Division of Geological and Geophysical Surveys Guidebook 1, p. 185-259.

Schmoll, H.R., Dobrovolny, Ernest, and Zenone, Chester, 1971, Generalized geologic map of the Eagle River-Birchwood area, Greater Anchorage Area Borough, Alaska: U.S. Geological Survey Open-file Map 71-248, 1 sheet, scale 1:25,000.

Theis, C.V., 1935, The relation between the lowering of the piezometric surface and the rate and duration of discharge of a well using ground-water storage: American Geophysical Union Transactions, v. 16, p. 519-524.

Zenone, Chester, Schmoll, H.R., and Dobrovolny, Ernest, 1974, Geology and ground water for land-use planning in the Eagle River-Chugiak area, Alaska: U.S. Geological Survey Open-file Report 74-57, 25 p.

CORRELATION OF GEOPHYSICAL WELL LOGS FOR A WATER DEVELOPMENT IN SOUTH ANCHORAGE, ALASKA

By L.L. Dearborn[1]

INTRODUCTION AND SETTING

At the request of the Municipality of Anchorage Water and Wastewater Utility, DGGS ran downhole geophysical logs at prospective production well 13 in south Anchorage (fig. 1). Three wells drilled within a 10-ft radius at the site—two test wells and a production well—reportedly did not penetrate the same aquifer, and projected water-supply capabilities varied greatly. These unexpected contradictions could not be explained in geologic or hydrologic terms that would allow a decision on where to place screens in the production well.

In ground-water studies, downhole geophysical logs are used to help interpret drill-log data (Campbell and Lehr, 1973). However, because these interpretations are commonly biased by downhole influences such as washouts, drilling-fluid invasion, and aquifer development, radiation logs of unconsolidated sedimentary materials are primarily used to refine the interpretation of an existing drill log.

The Anchorage lowlands are underlain by several sequences of Pleistocene till with interbedded outwash and fine-grained glaciolacustrine deposits up to 1,000 ft thick (Zenone and Anderson, 1978). Most outwash deposits are less than 50 ft thick and contain water hydraulically confined by the silty Bootlegger Cove Formation. In many high-yield production wells in the lowlands, screens are positioned in clean, coarse-grained beds within the outwash. Because these beds are discontinuous, the presence of highly productive aquifers is difficult to predict without considerable subsurface exploration (Zenone and Anderson, 1978).

The locations of four test wells and a production well are shown in figure 1. Test wells 2 and 3, which were not logged, are not considered pertinent to this report. Test wells 1 and 4 are cased with 6-in.-diam steel to 325 and 405 ft, respectively. Test well 1 was drilled by the cable-tool method and was perforated from 196 to 216 ft, 240 to 265 ft, and 304 to 324 ft. The perforated zones were developed and test-pumped before geophysical logging. Test well 4, drilled with an air-rotary rig, was not perforated. The prospective production well was lined with 16-in.-diam casing (also unperforated) to a depth of 360 ft; it too was drilled by the air-rotary method.

BASIC PRINCIPLES OF APPLIED RADIATION LOGGING

Three types of radiation logging—gamma-gamma, natural gamma, and neutron—were used in this investigation. Keys and MacCarey (1971) provide a more detailed description of the physics of radiation logging than presented below.

The gamma-gamma sonde measures relative differences in bulk density that result from gamma-photon bombardment from a cobalt isotope (^{60}Co), as detected by a sodium iodide crystal. All materials within the sphere of investigation, which includes about 6 in. of geologic material outside the casing, determine the intensity of backscattered gamma radiation detected by the crystal. On the log, this intensity, or bulk density, is highest where the recorded counts per second (cps) are lowest because of high absorption of radioactive energy.

Because no radioactive source is attached to the gamma sonde in a natural gamma log, only natural radiation emitted by geologic materials containing the isotopes ^{40}K, ^{238}U, and ^{232}Th is recorded. In the Anchorage area, clay and silt generally contain these isotopes, which account for most recorded gamma radiation. The count rate on the log is normally assumed to increase in direct proportion with the abundance of clay or silt in the material surrounding the casing.

In neutron logging, an americium isotope (^{241}Am) mixed with beryllium (Be) attached to a sonde emits neutrons that interact with geologic materials. The sonde responds primarily to the relative abundance of hydrogen atoms, which dissipates the energy to thermal levels (below 0.025 eV) more effectively than other elements. (Many neutrons are thermalized and do not travel back to the sonde's detector.) Thus, a low cps reading reflects a high hydrogen environment within several feet of the sonde. A neutron log represents 'total porosity' because it does not distinguish between water that is free to move and water that is either chemically bound or occupies isolated pore spaces. Consequently, clays—especially those that are not tightly compacted—commonly give a lower cps response than do sand-and-gravel aquifers.

[1]DGGS, P.O. Box 772116, Eagle River, Alaska 99577.

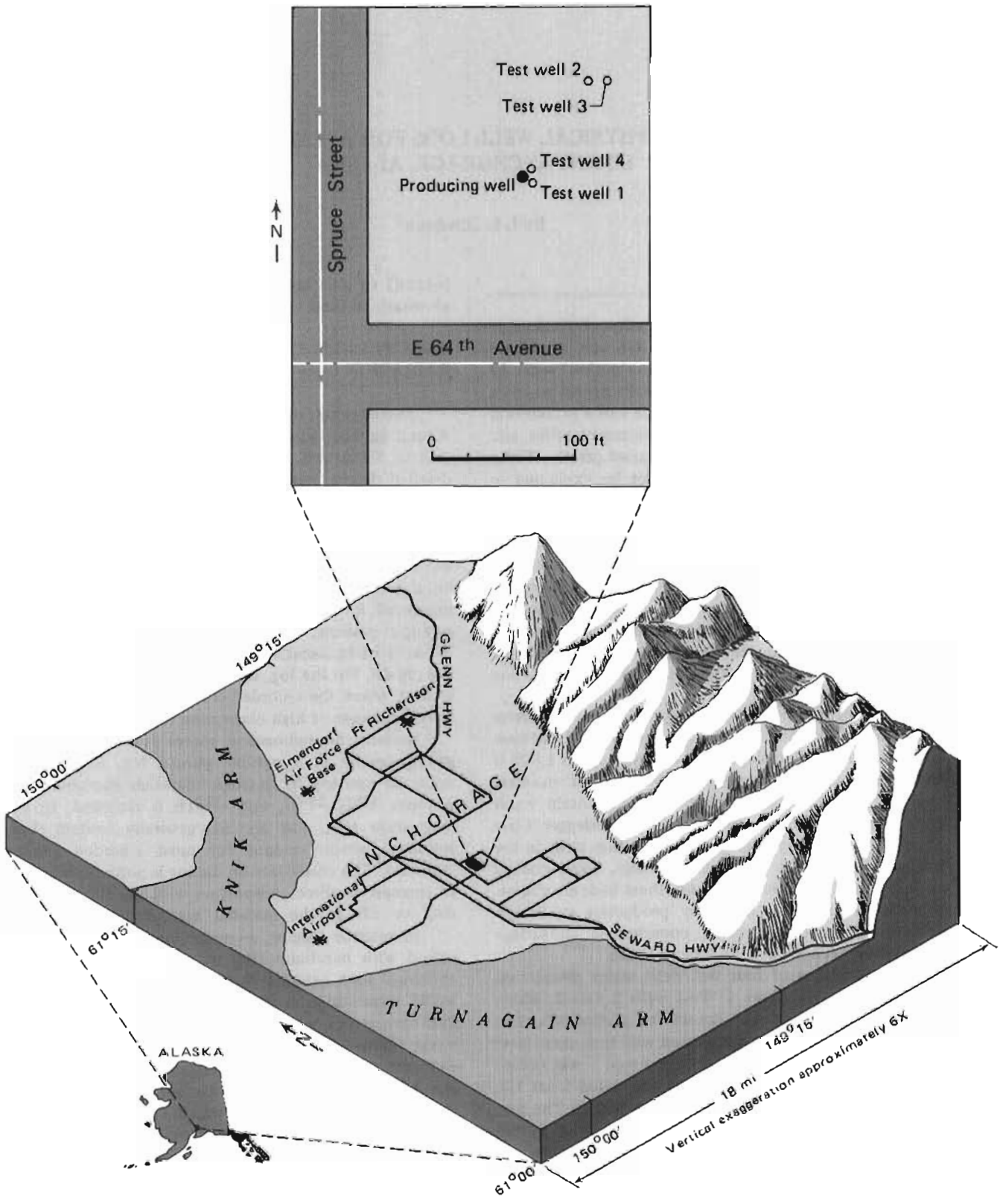

Figure 1. Location of Municipality of Anchorage well site 13.

The cps response of the sondes is affected by differences in casing diameter and thickness, by invasion of the sediments by drilling mud, and by turbidity of water within the casing. Such complications usually make quantitative correlation of logs from different wells impossible.

Washouts that sometimes occur just outside the well casing also interfere with log interpretation. A washout is an abrupt enlargement of the drillhole caused by the sloughing of loose sediments into the hole or by the erosive action of fluids during drilling. A pronounced bulk-density reduction (high cps) on the gamma-gamma log, high total porosity (low cps) on the neutron log, and relatively low natural gamma radiation generally indicate a washout. These log responses are partly a result of ground water replacing earth materials. Unless created by temporary deviations from normal drilling action of the bit, washouts can be a good indicator of the cohesiveness of a geologic unit.

INVESTIGATIVE APPROACH

The goal of the study was to show that geophysical logs of wells can be used to unscramble conflicting geologic descriptions in the well-drillers' logs (table 1) and to derive a truer profile of subsurface conditions. The basic assumption of the study was that all three wells penetrated a single lithologic sequence.

The radiation logs had to be qualitatively calibrated by standardizing geologic descriptions in the three drilling logs. To do so, the drillers' descriptions of each stratum were categorized into one of six hydrogeophysical units on the basis of typical responses for each log type and on geologic properties of these intervals that seemed distinctive to the drillers (table 2).

Because the tightness and cohesiveness of the matrix were commonly ambiguous, it was difficult to assign some geologic strata described by the drillers to a specific hydrogeophysical unit. For example, an interval described simply as 'clay and gravel' was assigned to unit 5, whereas it may actually consist of gravelly seams in the clay and belong in unit 4.

LOG-SUITE CORRELATIONS

Figure 2 shows three geophysical logs run in each of the wells and interpreted drillers' logs that were constructed using table 2 criteria. A hydrogeophysical profile (far right) represents a composite interpretation of all geophysical and drillers' logs. The upper 70 ft of sediments contained no significant aquifers and was not included in the study.

Initially, there seemed to be a lack of similarity, or correlation, across the log suite. The interpreted drillers' logs showed the same composition only at intervals from 194 to 197 and 319 to 328 ft. But, if tolerance is granted so as to include intervals that contain adjacent units in table 2, the interpreted logs may also be considered similar for the following intervals: 113-135, 144-147, 174-178, 243-251, 267-270, 274-278, and 294-309 ft. The total thickness of these intervals is 71 ft, or about one-fourth of the study interval spanned by all three wells.

By comparison, the radiation logs of the three wells exhibit readily apparent similarities at the following intervals: 70-78, 92-102, 204-223, 260-276, and 305-328 ft. Although the log of the last interval in the production well was disqualified (see p. 26), the total thickness of obvious geophysical correlations of the applicable study intervals is 76 ft, 5 ft more than the most liberal interpretation of the drillers' logs. More subtle similarities are apparent when the geophysical logs are compared with both hydrogeophysical logs and the original material descriptions by the driller. These comparisons led to the construction of the remaining correlation lines in figure 2, usually as an extension of a contact delineated by at least one driller.

DISCUSSION OF INTERPRETATIONS

Geophysical logs of the production well vary somewhat from apparent correlation patterns exhibited by the test wells, primarily because of the increased diameter and thickness of the casing. (Also, the sondes were not side-collimated, and log response may have been slightly biased by the varying distance between the moving sonde and the inside of the production-well casing; however, this factor was assumed to be negligible.) Because the casing is half again as thick as that of the test wells, deflections on the production-well logs exhibit less amplitude, and thus background fluctuations are more pronounced. Consequently, more interpretive emphasis was given to the test-well logs.

The most obvious discrepancy of the radiation-log correlations occurs between test wells 1 and 4 in the 140- to 147-ft stratum assigned to unit 4 in the interpretive profile (fig. 2). The gamma-gamma and neutron logs show that the relative bulk density is much less and that the apparent total porosity is much greater, respectively, for test well 4. The radiation logs of this well probably reflect a broad, washed-out zone that may encompass much of unit 2 (just above) and about one-third of unit 3 (below). Thus, no abrupt deflections on the logs of test well 4 appear at the 140- and 147-ft depths. This interval apparently did not wash out during drilling of test well 1, probably because the cable-tool drilling technique was used.

The 260- to 276-ft interval gave highly variable responses on all radiation logs and was assigned to unit 4 on the profile. This assignment is supported by the driller's log of the production well, which indicates beds of contrasting properties—probably silt or clay with sand and gravel seams—in the interval.

Log behavior strongly indicates that the major

Table 1. *Well-drillers' logs for Municipality of Anchorage well site 13.*[a]

Test well 1		Production well		Test well 4	
Depth (ft)	Description	Depth (ft)	Description	Depth (ft)	Description
0-3	Black peat	0-33	Unavailable	0-6	Fill and organics
3-26	Blue-gray silt, sand, gravel, and small boulders	33-50	Gray, gravelly hardpan	6-10	Tan, silty gravel
26-33	Blue-gray clay, sand, and gravel	50-55	Gravel, well takes water	10-15	Tan, damp, silty gravel
33-36	Blue-gray silty clay and fine sand	55-90	Gray, gravelly hardpan	15-18	Tan, silty gravel
36-48	Blue-gray silty clay embedded with sand and gravel	90-112	Tan, silty gravel, taking some water	18-30	Tan, silty gravel (water bearing)
48-53	Blue-gray silty clay and fine sand	112-123	Clay with gravel	30-60	Damp, gray, silty gravel
53-58	Blue-gray silty clay embedded with sand and gravel (water seeps)	123-135	Sandy clay and gravel, taking water	60-66	Gravel, water
58-64	Blue-gray fine to coarse sand; water	135-142	Sand and gravel	66-68	Gray clay
64-67	Blue-gray silty fine to coarse sand and fine to medium gravel, approximately 12 gpm	142-154	Clay with sand and gravel	68-80	Gray, sandy clay, water bearing
67-71	Blue-gray coarse sand and fine to medium gravel, water approximately 12 gpm	154-226	Unavailable	80-90	Gray, sandy clay and gravel, water bearing
71-76	Blue-gray, silty clay and fine sand	226-228	Gray silt with gravel	90-105	Water, sand, and gravel; 5 gpm SWL[b] at 100 ft = 28 ft
76-87	Blue-gray, silty clay embedded with sand and gravel (water seeps)	228-231	Tan, silty gravel, occasional boulders	105-140	Damp, tan clay and gravel
87-91	Tan and brown, fine to coarse sand and gravel	231-238	Gravel with cobbles, +3 in.	140-144	Tan sand and gravel; SWL at 144 ft = 33 ft
91-101	Tan and brown, silty clay embedded with water-bearing seams of sand and gravel	238-244	Tan, silty gravel with cobbles	144-147	Damp, tan clay and gravel
101-108	Tan silt and sand	244-252	Tan, silty sand and gravel	147-174	Tan sand and gravel; water

[a]DOWL Engineers (4040 B St., Anchorage) drawing, 'Municipality of Anchorage well 13 profile of holes 1 and 4,' dated January 14, 1982.
[b]Static water level as measured from the drilling datum.

Table 1 (con.)

Test well 1		Production well		Test well 4	
Depth (ft)	Description	Depth (ft)	Description	Depth (ft)	Description
108-121	Tan, silty clay embedded with sand and fine gravel	252-267	Tan, coarse sand and gravel, water	174-178	Damp, tan clay and gravel
121-146	Tan, silty clay embedded with seams of sand and gravel, seepage	267-270	Tan, silty gravel, occasional rocks	178-225	Tan sand and gravel; approximately 50 gpm at 198 ft; SWL at 180 ft = 35 ft, at 218 ft = 39 ft
146-164	Tan and brown, silty clay and fine sand (wet)	270-274	Brown clay and silt with gravel	225-251	Tan, silty gravel (water weeping)
164-169	Tan and brown, silty clay and sand embedded with gravel	274-285	Tan clay and silt with gravel and rock, hardpan	251-266	Tan sand and gravel; water
169-189	Tan and brown, silty clay and sand embedded with gravel, seepage	285-292	Tan clay and silt with cobbles, +3 in., some gravel	266-318	Tan, silty gravel (water weeping)
189-192	Brown and gray, fine to coarse sand and gravel	292-294	Gray clay with gravel and rocks	318-328	Tan gravel, 10 to 30 gpm; SWL at 321 ft = 53 ft
192-220	Brown cemented sand and gravel (seeps of water)	294-299	Cobbles with gray clay, cemented, trace gravel	328-330	Tan, silty gravel (water bearing)
220-226	Tan and gray, silty clay embedded with fine to coarse sand and gravel	299-309	Gray clay with gravel and rock, hardpan	330-357	Tan sand and gravel, approximately 50 gpm; SWL at 340 ft = 55 ft
226-238	Tan, brown, and gray clay embedded with sand, gravel, and boulders	309-319	Gravel with gray clay	357-377	Tan, silty gravel, no water
238-273	Blue, green, and brown, fine to coarse sand and gravel cemented with tan clay	319-329	Sand and gravel, water with tan clay	377-380	Tan, silty, sandy gravel, approximately 10 gpm; SWL at 380 ft = 55 ft
273-289	Tan and gray clay embedded with sand, gravel, and boulders (trace of water)	329-336	Gravel and rocks with tan clay; water	380-405	Tan, gravelly hardpan, seeping water
289-325	Sand, gravel, and boulders cemented with tan clay	336-344	Gravelly clay, open hole possible, tan clay		
		344-360	Tight sand mixed with gravelly clay, open hole, no apparent water at 345 ft		

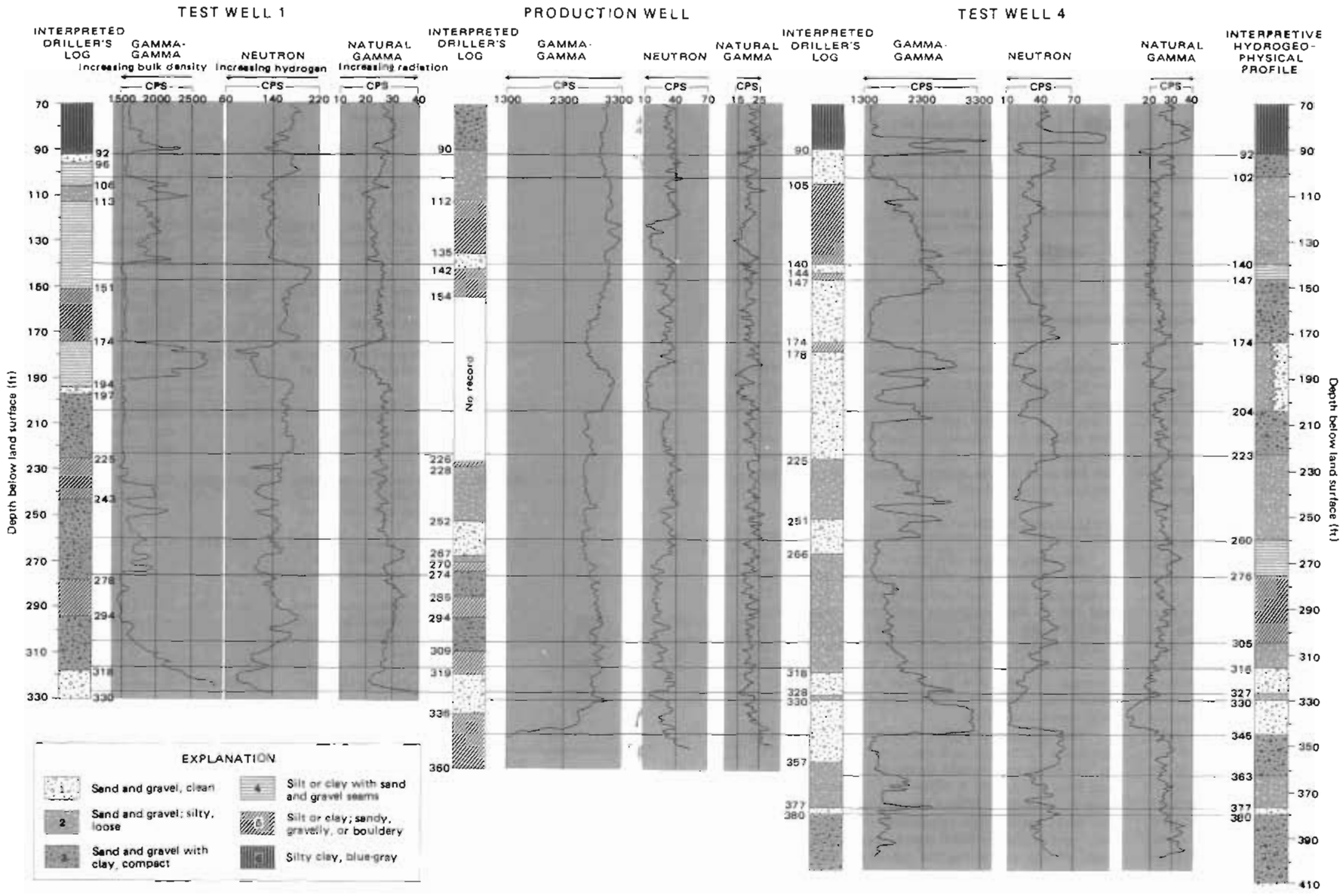

Figure 2. Well-log correlations and interpretation.

Table 2. *Characterization of radiation-log responses for designated hydrogeophysical units at development site (in descending order of water-yielding potential).*

Hydrogeophysical units	Relative radiation-log response[a]									Geologic composition as inferred from driller's material logs	Water-yielding potential (inferred)
	Gamma-gamma (cps →)			Neutron (cps →)			Nat. gamma (cps →)				
	L	M	H	L	M	H	L	M	H		
1										Sand and gravel, clean	Medium-high (good aquifer)
2										Sand and gravel; silty loose	Low-medium (marginal aquifer)
3										Sand and gravel with silt and clay, compact	Very low-low (seepage in places)
4										Silt or clay with sand and gravel seams	None-low (highly variable)
5										Silt or clay, sand, gravelly, or bouldery	Very low
6										Silty clay, blue-gray	None

[a]Radiation level: L - low, M - moderate, H - high; ◀ points away from predominate level.

aquifer at this development site is located at about 316 to 345 ft. Furthermore, gamma-gamma and neutron logs of test well 4 suggest the presence of a loose, moderate- to high-porosity zone beginning at 330 ft, which is typical of a clean sand-and-gravel aquifer of relatively uniform texture. Production-well logs show contradictory trends because of residual drilling mud in the well. The mud gradually thickened with increasing depth, eventually limiting logging depth to 350 ft, 10 ft from the bottom.

The interpretive profile shows a second aquifer, with radiation-log characteristics of both units 1 and 2, at 174 to 204 ft below land surface. The driller's log of test well 4 suggests that this interval (along with most of the hole below 140 ft) is of unit-1 or unit-2 composition. However, the driller of test well 1 described the lithology so differently that only one 3-ft-thick layer could be termed either unit 1 or 2. This aquifer—and most other intervals assigned to unit 2 in the profile—seemingly consists of interbedded loose and compacted sediments, each capable of yielding highly variable amounts of water. Furthermore, the driller of test well 1 frequently described unit-2 geologic material on the profile as unit 3. The reverse is found in logs of the production well and test well 4. The primary distinction between units 2 and 3, based on geophysical-log interpretation, is that unit 3 is slightly more indurated, resulting in lower cps on the gamma-gamma log. Again, different drilling methods probably account for the varying lithologic descriptions: the cable-tool operator (test well 1) noted more fines and more drilling resistance than did the air-rotary driller (test well 4) who used more powerful equipment.

It is not surprising that the application of table 2 resulted in an interpretive hydrogeophysical profile with several depth intervals that do not match unit designations assigned to the drillers' logs. In actuality, the character of adjacent units within table 2 may differ only slightly from one another, and radiation responses may not be unique for one or more units. Nevertheless, the full suite of logs generally supports the hydrogeophysical units as defined.

WELL COMPLETION AND TEST RESULTS

My interpretation of a suite of three radiation logs in each of three wells, with reference to drillers' logs, delineated a major sand-and-gravel aquifer between 316 and 345 ft. Gamma-gamma and neutron logs indicate that the lower part of the aquifer (below 330 ft) has the highest porosity and should produce the most water per ft of screen. Also, there appears to be a weaker aquifer between 174 and 204 ft; natural gamma and gamma-gamma logs suggest that this aquifer contains more fines than does the lower one.

The interpreted aquifer depths were conveyed to the Water Utility and its design consultants. Later, 0.15-in. slot-width screens were installed from 189 to 220 ft and from 309 to 335 ft below land surface. Some fines were removed from around the outside of the screens in the lower aquifer with compressed air. The increase in well yield was much lower than expected, and because a yield of only several hundred gallons per minute (gpm) was achieved, the lower aquifer was abandoned (Dee High, DOWL Engineers, oral commun., March 1983), and this section of the well was backfilled.

The upper aquifer responded sluggishly to development, but eventually well yield improved markedly with

air surging. A strong chlorine solution was used to break down additives in the drilling fluid. Eventually, this aquifer was air pumped at 1,780 gpm for 7 hr, resulting in a pumping water level of 143 ft, or 96 ft of drawdown (High, oral commun., March 1983). Water-level recovery in the well was fairly rapid.

A minor aquifer at an approximate depth of 250 to 265 ft was air pumped at up to 35 gpm in each of the test wells. The hydrogeophysical characteristics interpreted from the radiation logs of this interval suggest that water yield should be considerably less than for the other identified aquifers.

In summary, the drillers' logs have been remolded into a single log of the subsurface through radiation logging. Even though complicated by differences in drilling methods and well construction, the composite log suite represents a logical correlation of the geological contacts recorded by one or more drillers with those separating defined hydrogeophysical units. Because of the objective nature of geophysical sensing, the hydrogeophysical profile constructed from the combined drillers' logs and borehole geophysical logs depicts aquifers more accurately at this site than do drillers' logs alone. The intervals chosen for screening encompassed part of the aquifer zones defined by this analysis. Production testing of the upper screened zone confirmed a high-yield aquifer. However, a lack of similar results from the lower aquifer is probably due to inadequate flushing of drilling fluids and possibly placing the screen 5 to 10 ft too high.

ACKNOWLEDGMENTS

I thank the Municipality of Anchorage Water and Wastewater Utility for the opportunity to log their wells. The support given by DOWL Engineers of Anchorage in providing drillers' logs and for on-site preparation for logging is greatly appreciated. Valuable reviews were provided by J.A. Munter (DGGS) and Tom Williams (DOWL Engineers).

REFERENCES CITED

Campbell, M.D., and Lehr, J.H., 1973, Water well technology: New York, McGraw Hill, 681 p.

Keys, W.S., and MacCarey, L.M., 1971, Application of borehole geophysics to water-resources investigations, Chapter E1: U.S. Geological Survey Techniques of Water Resources Investigations Report TW 12-E1, 126 p.

Zenone, Chester, and Anderson, G.S., 1978, Summary appraisals of the nation's ground-water resources - Alaska: U.S. Geological Survey Professional Paper 813-P, 28 p.

GARNET COMPOSITIONAL ESTIMATES AS INDICATORS OF PROGRESSIVE REGIONAL METAMORPHISM IN POLYMETAMORPHIC ROCKS, KANTISHNA HILLS, ALASKA.

By T.K. Bundtzen[1] and N.C. Veach[1]

INTRODUCTION

Prograde mineral assemblages in rocks of basic composition and other mineralogical and textural criteria (Bundtzen, 1981) indicate that polymetamorphic basement schist in the Kantishna Hills, Alaska (fig. 1), has undergone progressive regional metamorphism. Interbedded pelitic and quartzo-feldspathic schists contain mineral assemblages compatible with this conclusion, but do not alone provide definitive evidence.

By using techniques described by Winchell (1958) and Deer and others (1967), garnet porphyroblasts were extracted from quartzo-feldspathic schist to obtain five end-member compositional estimates. We believe these chemical compositions may further document relative metamorphic grade, especially in the quartzo-feldspathic units, where mineral assemblages are compatible with but not definitive for a metamorphic-facies assignment. These analyses and their implications concerning regional metamorphism are summarized.

GEOLOGIC SETTING

The Kantishna Hills consists of four regionally metamorphosed Precambrian to upper Paleozoic rock units: a) a basement schist, informally referred to as the Birch Creek Schist,[2] b) the Spruce Creek Sequence,[3] c) the Keevy Peak Formation, and d) the Totatlanika Schist (fig. 2). Collectively, these rocks form a small part of the Yukon Crystalline Terrane (Tempelman-Kluit, 1976), which covers several hundred thousand square kilometers in northern Canada and interior Alaska.

The metamorphic petrology, age, and distribution of these units are described by Bundtzen and Turner (1979) and Bundtzen (1981). The oldest rock unit, the Birch Creek Schist of Precambrian age, consists of variable amounts of greenstone, greenschist, micaceous quartzite, calcareous and graphitic schist, quartzo-feldspathic schist, gneiss, and marble. Mineralogical, textural, and radiometric-age evidence indicate a polymetamorphic history for the Birch Creek Schist. In many thin-section samples of the unit, mineral assemblages in disequilibrium are recognizable. Mineralogical criteria indicate that a prograde amphibolite-facies mineral assemblage was retrogressively metamorphosed to the lower greenschist facies. Prograde and retrograde assemblages are summarized in table 1. Mineral assemblages in rocks of basic composition provide the best evidence of metamorphic grade in the prograde event. Detailed petrographic studies enabled Bundtzen (1981) to construct progressive biotite, garnet, hornblende, and calcic-plagioclase isograds in a 12-km-wide, northwest-trending belt in the southern part of the study area (fig. 2). Using criteria established by Turner (1968), the appearance of hornblende and calcic plagioclase (An $\geq$ 17) in basic rocks in the study area indicates the amphibolite facies of regional metamorphism. Although prograde mineral assemblages in interbedded quartzo-feldspathic schist and gneiss are compatible with the amphibolite-facies designation, they do not alone provide a definitive metamorphic-facies classification.

Structural and textural changes also support the progressive metamorphic gradient. From southeast to northwest, rock textures evolve from flaser 'tectonic' fabrics to complete, uniform recrystallization. Garnet, amphibole, and feldspar porphyroblasts increase in size in the same direction.

Table 1. *Mineral assemblages from Birch Creek schist, Kantishna Hills, Alaska (Bundtzen, 1981).*

Pelitic and quartzo-feldspathic schists and impure quartzite

1. Northwest part of study area (66 thin sections). Prograde: oligoclase-andesine + garnet + white mica ± hornblende + biotite. Retrograde: albite + zoisite/clinozoisite + chlorite + phengitic white mica + biotite ± calcite

2. Southeast part of study area (22 thin sections). Prograde: biotite + white mica ± garnet + albite-oligoclase(?). Retrograde: chlorite + zoisite + microcline + albite. Tourmaline, zircon, and quartz present in all samples.

[1]DGGS, Fairbanks, Alaska 99701.

[2]Foster and others (1973) suggested the term 'Birch Creek Schist' be abandoned. However, Bundtzen (1981) retained the term for rock units that have undergone two or more periods of recrystallization and form basement, consistent with the Mertie (1937) definition.

[3]Informal name for belt of metavolcanic and metasedimentary rocks that host strata-bound and crosscutting vein and precious-metal deposits in the Kantishna mining district.

Table 1. *(con.)*

Amphibolite and greenschist

1. Northwest part of study area (25 thin sections). Prograde: oligoclase-andesine + hornblende + garnet + biotite ± white mica + sphene. Retrograde: albite + zoisite/clinozoisite + chlorite + biotite ± actinolite ± calcite.

2. Southeast part of study area (6 thin sections). Prograde: albite + actinolite + garnet ± biotite + sphene. Retrograde: albite + zoisite/clinozoisite + chlorite ± calcite. Sphene and quartz present in all samples.

Calcareous schist and marble

1. Northwest part of study area (2 thin sections). Tremolite + diopside + albite + epidote + tourmaline + calcite + quartz.

2. Remainder of study area (5 thin sections). White mica + calcite ± quartz + chlorite. Prograde and retrograde assemblages not determined for calcareous rocks.

ANALYTICAL METHODS

Samples of quartzo-feldspathic schist containing garnet-biotite-white mica-hornblende-plagioclase assemblages were selected from 10 sites in the study area. Care was taken to select samples with large, fresh (> 1 cm diam) garnet porphyroblasts. Thin-section examinations show the garnets were largely unaffected by retrograde metamorphism and relatively free of mineralogical inclusions.

Physical properties of each garnet separate were measured. The refractive indices were determined by using index-refraction immersion liquids, a refractometer, and a polarizing microscope. Lattice or unit-cell-edge constants were determined by an X-ray diffractometer that measured d-spacings on powder patterns (1/4 degree per min slow scanning). Lattice indexes (h,k,l) are based on an isometric unit-cell-edge constant ($a=d\sqrt{h^2+k^2+l^2}$), where 'a' is the unit-cell edge in angstroms, 'd' is the lattice spacing, and 'h,' 'k,' and 'l' are the lattice indices. The value of 'a' is an average of three slow-scanning powder patterns per sample. Specific-gravity values were the most difficult to determine. Inclusion-free grains were measured on a Berman density balance that averaged grain weights from 10 to 25 g. The percentage of manganese oxide was determined by atomic-absorption spectrophotometry of aqueous solutions prepared by lithium metaborate fusion.

These physical properties were compared with published graphs and tables that relate physical properties of garnets to their composition. According to Hutchison (1974), most garnets formed during regional metamorphism may be considered five-component

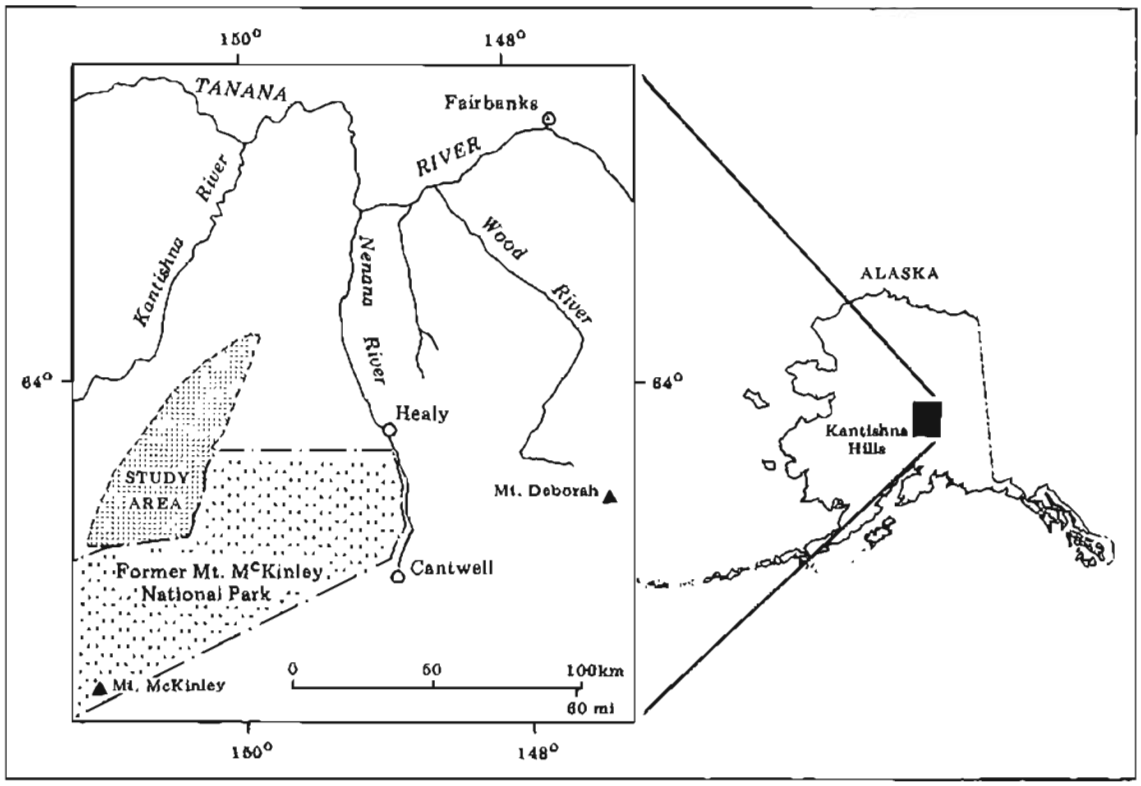

Figure 1. Location map of the Kantishna Hills, Alaska.

systems in terms of almandine, andradite, grossular, pyrope, and spessartine content. Skinner (1956) determined the refractive index, unit-cell edge, and specific gravity of five synthetically produced garnet end members. Assuming that linear variance corresponds directly with chemical change, Winchell (1958) incorporated Skinner's data and showed that four-component garnet compositions can be estimated on a ternary diagram

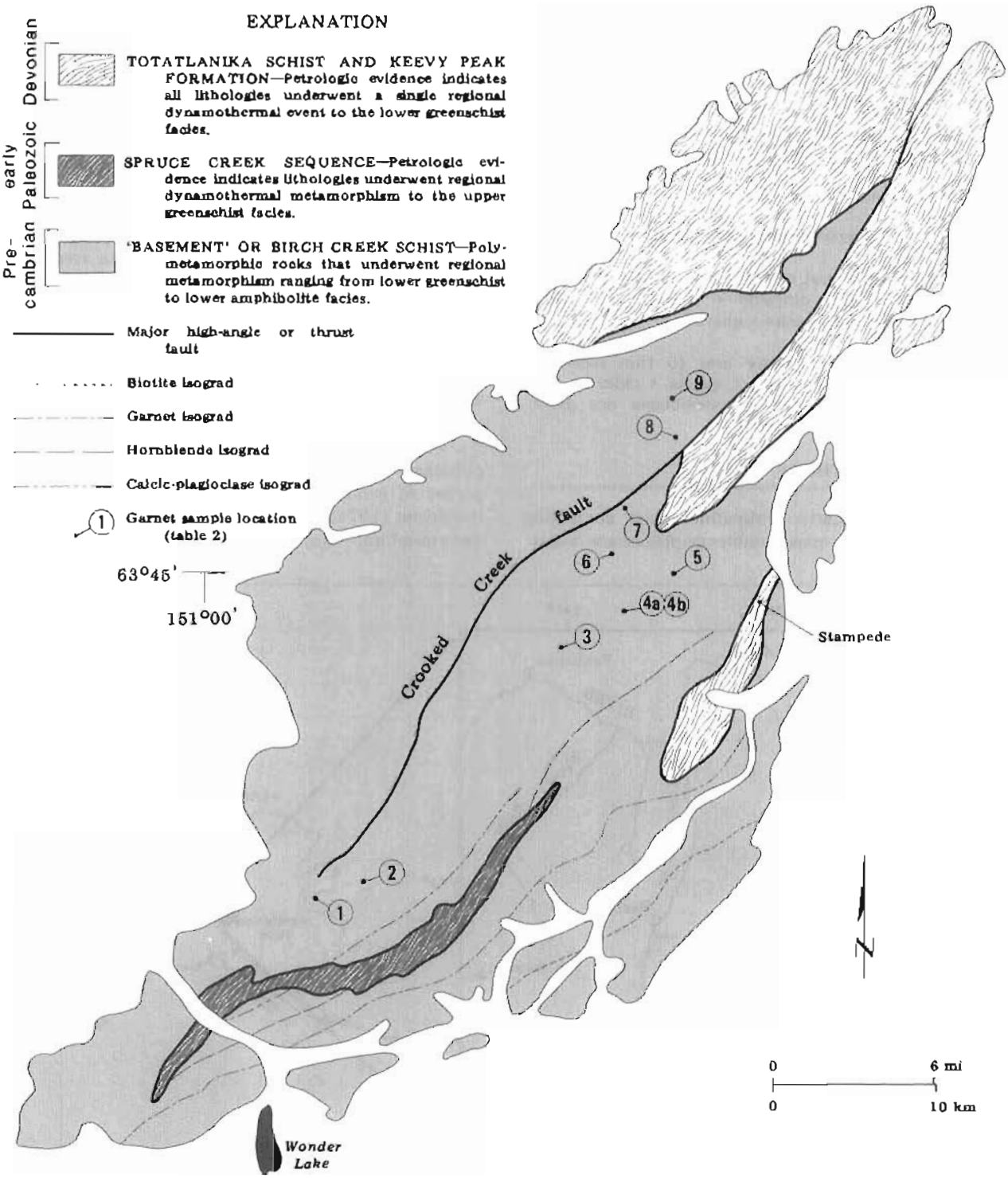

Figure 2. Map showing crystalline rocks in the Kantishna Hills, with mineral isograds and garnet-sample locations in the Birch Creek Schist. From Bundtzen (1981).

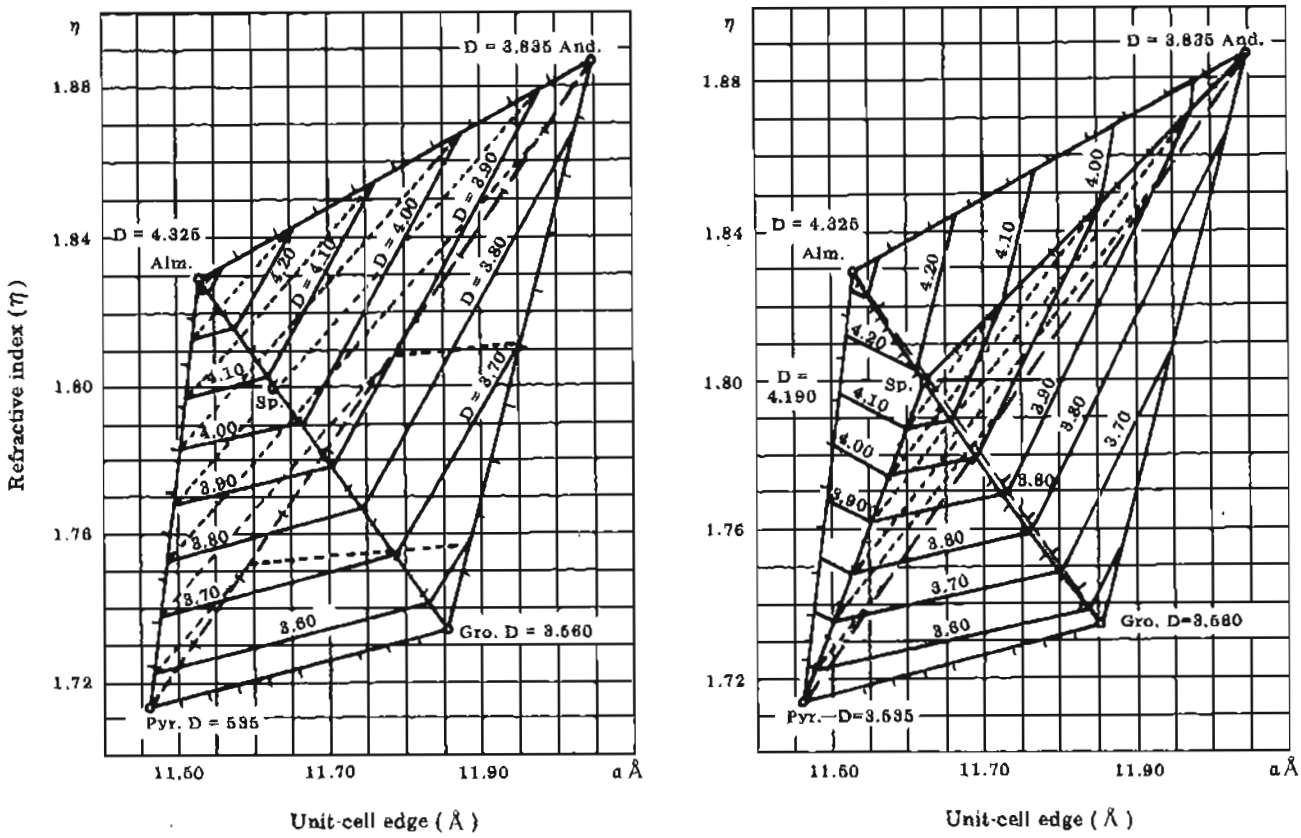

Figure 3. Determinative charts for garnets. From Winchell (1958).

where the refractive index and the unit-cell edge are ordinate and abscissa, respectively, and specific gravity is projected into the third dimension (fig. 3). Using these physical properties, Deer and others (1967) compared the value of percent manganese oxide of the unknown garnet with the computed percent manganese oxide of spessartine and obtained a five-component system.

The mole-percent end members of garnets using the refractive index, unit-cell edge, specific gravity, and percent manganese oxide (according to Winchell, 1958) are shown in table 2. These compositional estimates are approximate because of limiting factors such as retrograde chemical changes and mineralogical inclusions. Three garnets determined by this method were analyzed for major oxides (table 3). With some adjustments in pyrope content, the actual oxide values, when computed to end-member compositions, agree with those obtained by the method of Deer and others (1967).

In the study area, garnets formed by prograde regional metamorphism of the Birch Creek Schist are dominantly almandine.

INTERPRETATION OF DATA

Garnets undergo readjustment of ion assemblages under mechanical and thermal stress. Ion substitutions within garnet structures are affected by temperature and pressure. Increasing pressure favors the presence of smaller ions, whereas increasing temperature favors larger ions.

Turner (1968) drew attention to the significance of the order of appearance of index minerals in different metamorphic terranes. An early appearance of almandine garnet is indicative of high-pressure regional metamorphism. According to Bundtzen (1981), the order of appearance of index minerals in the Kantishna Hills (biotite-almandine-hornblende/plagioclase) is comparable with the schists of East Otago, New Zealand, a belt of relatively high-pressure regional metamorphism. Hence, we can expect larger ionic radii of Ca++ and Mn++ (0.99 and 0.80 Å, respectively) to be replaced with Fe++ and Mg++ (0.74 and 0.66 Å) during progressive regional metamorphism in the study area.

Nandi (1967) compiled garnet compositional data (N=84) and showed that the FeO + MgO varies inversely in linear fashion with CaO + MnO from garnets collected within sillimanite, kyanite, and garnet isograds of pelitic metamorphosed rocks. For almost every sample, an

Table 2. *Estimates of garnet compositions from the Kantishna Hills, Alaska, after methods described by Deer and others (1967, p. 21-31).*

Map no. (fig. 2)	Field no.	Sample type	Mole-percent end members of garnet[a]					Unit-cell edge (Å)	Specific gravity	Index of refraction	MnO (%)
1	75Ast2900	Biotite-muscovite schist	Al-56.8	An-20.5	Gr-15.9	Sp-5.6	Py-1.2	11.630	3.45	1.806	2.40
2	75Ast1857b	Garnet amphibolite	An-68.4	Gr-15.5	Sp-10.3	Py-3.9	Al-1.9	11.636	3.86	1.808	4.45
3	76BT171	Quartzo-feldspathic schist	Al-71.9	Py-11.0	An-10.0	Gr-6.9	Sp-0.2	11.591	4.14	1.817	0.43
4a	75Ast64a	Quartzo-feldspathic schist	Al-57.5	Gr-27.7	Al-9.2	Py-3.6	Sp-2.0	11.615	3.85	1.808	0.85
4b	75Ast64b	Amphibolite	Al-59.6	Gr-27.9	An-8.3	Sp-2 5	Py-1.7	11.627	3.83	1.808	1.10
5	76BT273	Quartzo-feldspathic schist	Al-71.5	Gr-13.3	An-7.2	Py-6.3	Sp-1.7	11.609	4.13	1.813	1.74
6	75Ast1598b	"	Al-64.6	Py-15.1	An-11.1	Gr-8.7	Sp-0.5	11.598	4.09	1.810	0.96
7	75Ast5	"	Al-66.6	Py-14.1	An-11.1	Gr-7.7	Sp-0.5	11.599	4.10	1.813	1.23
8	76BT253	"	Al-64.8	An-24.1	Gr-8.0	Sp-1.7	Py-1.4	11.624	3.75	1.806	0.75
9	76BT258	"	Al-62 7	Py-17.1	An-12.0	Gr-7.8	Sp-0.4	11.603	4.07	1.810	0.78

[a]Al - almandine, An - andradite, Gr - grossular, Py - pyrope, Sp - spessartine.

Table 3. *Major-oxide data for garnet separates, Birch Creek Schist, Kantishna Hills, Alaska.*

Map no. (fig. 2)	Major oxides							Cation ratios used in figures 4 and 5		
	SiO_2	Al_2O_3	CaO	MgO	Fe_2O_3	FeO	MnO	FeO+MgO / CaO+MnO	CaO+MnO	FeO+MgO
1	36.78	16.70	12.70	0.36	6.46	24.59	2.40	1.6523	15.10	24.95
2	36.67	7.02	28.35	1.16	21.55	0.82	4.45	0.0604	32.80	1.98
3	37.34	19.14	5.87	3.28	3.15	31.13	0.43	5.4619	6.30	34.41
	35.10	19.17	5.12	1.16	3.73	33.16	0.48	6.1285	6.50	34.32
4a	37.51	19.40	13.37	1.07	2.90	24.90	0.85	1.8263	14.22	25.97
4b	37.36	19.50	13.15	0.51	2.61	25.81	1.10	1.8470	14.25	26.32
5	37.20	19.63	7.34	1.88	2.27	30.97	1.74	3.6167	9.08	32.84
	34.17	19.71	6.83	0.89	2.43	32.37	1.91	3.8055	8.74	33.26
6	37.75	19.15	6.91	4.50	3.50	27.97	0.96	4.1258	7.87	32.47
7	37.63	19.08	6.53	4.20	3.50	28.84	1.23	4.2577	7.76	33.04
	38.48	18.46	6.01	1.09	3.92	28.73	0.80	4.3789	6.81	29.82
8	36.47	15.81	10.93	0.42	7.59	28.06	0.75	2.4384	11.68	28.48
9	37.89	19.04	6.87	5.10	3.78	27.15	0.78	4.2157	7.65	32.25

[a]Major oxides calculated from mole-percent end members in table 2.
[b]Analyses by X-ray fluorescence, Technical Service Laboratories, Mississauga, Ontario.

increase in FeO + MgO correlates with increasing metamorphic grade. Nandi (1967) also demonstrated a positive correlation with decreasing unit-cell size and increasing pressure-temperature (PT) conditions.

Garnet compositional estimates from the study area were plotted on a Nandi (1967) FeO + MgO versus CaO + MnO diagram. The comparison shows that FeO + MgO increase linearly to the northwest in the study area. Four garnets near Stampede plot within the garnet zone of metamorphism, whereas five near Crooked Creek plot in the kyanite zone of metamorphism (figs. 2 and 4).

An independently derived hyberbolic relationship is illustrated when samples are plotted on a unit-cell-edge versus FeO + MgO/CaO + MnO variation diagram (fig. 5). Six of 10 Kantishna garnets plot in the garnet zone of metamorphism and four plot in the kyanite zone of metamorphism. Except for sample 9 (table 2), all fall within the fields shown in figure 4; sample 9 plots on the garnet-kyanite zonal boundary (fig. 5).

In both diagrams, garnets from the study area show increasing amounts of FeO + MgO and a decreasing unit-cell edge in a northwesterly direction, which suggests increasing regional metamorphic grade in that direction. Samples 8 and 9 break from the pattern of a progressive decrease in unit-cell size and FeO + MgO content to the northwest. Both are found north of the Crooked Creek fault zone, which suggests that different pressure-temperature conditions have existed in the regionally metamorphosed rocks there.

DISCUSSION

Stanton and Williams (1978), Evans (1965), and Miyashiro and Shido (1973) discuss the use of garnet composition as an indicator of regional metamorphism and conclude that host-rock composition, diffusion rates in garnet, oxygen fugacity, and fluid phase of metamorphism are important controlling factors for garnet compositions.

In our study, we attempted to analyze garnet from rocks of the same composition. All samples except 4b (table 2) were derived from quartzo-feldspathic schists of similar mineralogical and chemical compositions. Two garnets from rocks of amphibolite and quartzo-feldspathic schist from the same locality (samples 4a,b, table 2) show similar compositions.

We emphasize that our garnet compositions are estimated by indirect physically measured properties and limited oxide analyses. Additionally, the nonuniform sample spacing in the study area constrains interpretations to generalizations. Furthermore, the Nandi (1967) work is based on garnets extracted from pelitic rocks rather than quartzo-feldspathic schists.

In summary, our data show calcium-rich garnets in the southeast part of the study area and iron-magnesium-rich garnets in the northwest. These results are compatible with mineralogical, structural, and textural evidence (previously cited) that indicates a progressive northwest-trending increase in PT conditions during

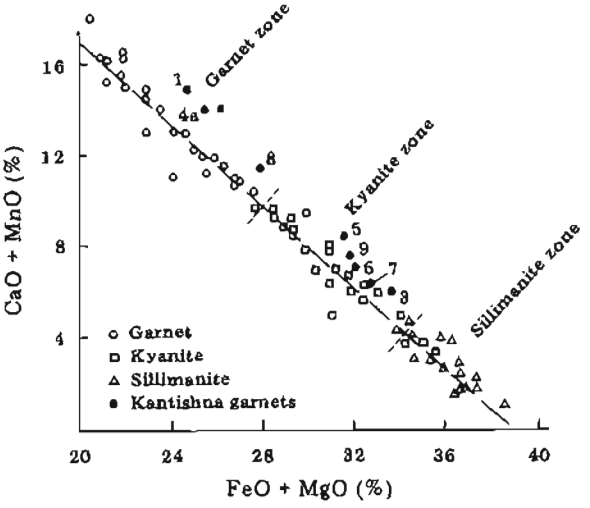

Figure 4. (CaO + MnO)-(FeO + MgO) variation diagram for garnets of different metamorphic grade. From Nandi (1967).

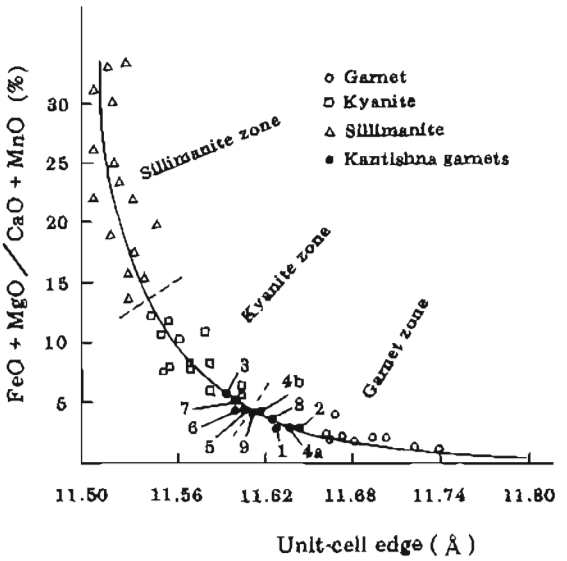

Figure 5. Variation of FeO + MgO)/(CaO + MnO) ratio with unit-cell edge for garnets. From Nandi (1967).

prograde regional metamorphism in the Birch Creek Schist in the Kantishna Hills.

ACKNOWLEDGMENTS

The authors thank D.B. Hawkins (University of Alaska) and J.T. Dillon (DGGS) for their constructive reviews of the manuscript, and Hawkins for continuous aid and encouragement during laboratory investigations.

REFERENCES CITED

Bundtzen, T.K., 1981, Geology and mineral deposits of the Kantishna Hills, Mt. McKinley Quadrangle, Alaska: Fairbanks, University of Alaska unpublished M.S. thesis, 237 p.

Bundtzen, T.K., and Turner, D.L., 1979, Geochronology of metamorphic and igneous rocks in the Kantishna Hills, Alaska, *in* Short notes on Alaskan Geology - 1978: Alaska Division of Geological and Geophysical Surveys Geological Report 61, p. 25-30.

Deer, W.A., Howie, R.A., and Zussman, T., 1966, An introduction to the rock-forming minerals: New York, Wiley and Sons, p. 80 84.

Evans, B.W., 1965, Pyrope garnet -- a piezometer or thermometer?: Geological Society of America Bulletin, v. 76, no. 8, p. 1295-1299.

Foster, H.L., Weber, F.R., Forbes, R.B., and Brabb, E.E., 1973, Regional geology of the Yukon-Tanana Upland, Alaska: American Association of Petroleum Geologists Memoir 19, p. 388-395.

Hutchinson, C.S., 1974, Laboratory handbook of petrographic techniques: New York, London, Sydney, Toronto, Wiley and Sons, 527 p.

Mertie, J.B., Jr., 1937, Geology of the Yukon-Tanana region: U.S. Geological Survey Bulletin 872, 250 p.

Miyashiro, A., and Shido, F., 1973, Progressive compositional change of garnet in metapelite: Lithos, v. 6, p. 13-20.

Morrison, D.H., 1964, Geology and ore deposits of Kantishna and vicinity: Fairbanks, University of Alaska unpublished M.S. thesis, 100 p.

Nandi, K., 1967, Garnets as indices of progressive regional metamorphism: Mineral Magazine, v. 36, no. 3, p. 89-93.

Skinner, B.J., 1956, Physical properties of end-members of the garnet groups: American Mineralogist, v. 41, no. 5, p. 428-436.

Stanton, R.L., and Williams, K.L., 1978, Garnet compositions at Broken Hill, New South Wales, as indicators of metamorphic processes: Journal of Petrology, v. 19, no. 3, p. 514-529.

Templeman-Kluit, D.J., 1976, The Yukon Crystalline Terrane: Enigma in the Canadian Cordillera: Geological Society of America Bulletin, v. 87, no. 9, p. 1343-1357.

Turner, F.J., 1968, Metamorphic petrology: New York, McGraw Hill, 401 p.

Winchell, A.N., 1958, The composition and physical properties of garnet: American Mineralogist, v. 43, p. 595-600.

GEOLOGY OF THE MISS MOLLY MOLYBDENUM PROSPECT, TYONEK C-6 QUADRANGLE, ALASKA

By Gregory Fernette[1] and Gaylord Cleveland[2]

INTRODUCTION

The Miss Molly molybdenum prospect, also known as the Hayes Glacier prospect, is located in the Alaska Range about 80 mi northwest of Anchorage, near the toe of the Trimble Glacier in the Tyonek C-6 Quadrangle (fig. 1). The prospect was first staked in 1959 by Glacier Mining Company and restaked in 1979 by Donald and Virginia Hawick of Anchorage. Only brief descriptions of the site are available in the literature (Berg and Cobb, 1967; Hollister, 1978).

This paper is based on a 5-day field examination completed in August 1979 (Cleveland and others, 1979). Most of the property is covered by glacial debris and dense vegetation, with good bedrock exposures only along the Trimble River (fig. 2) and in a few tributary stream valleys.

REGIONAL GEOLOGIC SETTING

The prospect is located near the eastern margin of the Alaska - Aleutian Range batholith, which in this area is early Tertiary in age with amphibole and mica age dates that range from 59 to 56 m.y. (Reed and Lanphere, 1973). Country rocks in the area are Jurassic to Cretaceous graywacke, siltstone, chert, and lesser intermediate to mafic volcanic rocks (Magoon and others, 1976).

PROPERTY GEOLOGY

The Miss Molly property is underlain by a 1.5-mi-wide granitic stock that is elongate to the northwest and intrudes thin-bedded siltstone (fig. 3a). The northwest end of the stock extends beyond the map area; the southeastern end of the pluton probably terminates beneath alluvial gravels in Trimble River valley. Exposed intrusive contacts are steeply dipping and locally offset by small faults. The granite displays several well-developed joint sets, some of which contain mineralized veins.

The stock is composed of leucocratic, phaneritic, equigranular biotite granite. Hand-specimen examination indicates an average composition of roughly 25 percent quartz, 72 percent feldspar, and 3 percent biotite. Locally the biotite content is less than 1 percent, but otherwise the stock is fairly uniform in composition. No porphyritic phases were noted. Whole-rock analysis of a relatively unaltered sample (table 1) indicates a granitic composition. However, the aluminum, sodium, and potassium are relatively low and the silica high for a typical granite. T.K. Bundtzen (written commun., 1983) suggests that the sample may have been enriched in silica after crystallization. Granitic dikes identical in texture to the main phase of the stock and several thin, tourmaline-bearing aplite dikes intrude the country rock along the southern contact of the stock. Molybdenum values (3 to 19 ppm) in samples of unaltered granite are significantly higher than those of average granites (Hawkes and Webb, 1962).

Country rock at the property consists of highly folded, thin-bedded brown siltstone that is metamorphosed to dark-purple-gray biotite hornfels near intrusive contacts. The hornfels locally contains 0.5 to 1 percent pyrite and pyrrhotite.

MINERALIZATION AND ALTERATION

Alteration and mineralization occur in two intersecting linear features—the Trimble River and West mineralized zones—that form an 'L' along the south side of the pluton (fig. 3). The Trimble River zone is well exposed in the southeastern part of the property and was mapped and sampled in detail. The West zone was examined during a single traverse only.

Near the southeast contact of the stock, the Trimble River zone extends northeast for at least 1,800 ft and is 200 to 500 ft wide. Molybdenite mineralization occurs in regularly spaced, subparallel, planar quartz veins ranging from 1/2 to over 14 in. wide and spaced 5 to 30 ft apart (fig. 4). The veins strike N. 10°-40° W., nearly perpendicular to the trend of the zone, and dip steeply (80°) to the northeast and southwest. The veins fill joints and less commonly shears and locally bifurcate along strike. The most abundant vein mineral is white to clear, banded, coarsely crystalline quartz; the texture is indicative of open-space filling. Dark-gray quartz is present in some veins. Pyrite is disseminated in most veins, but rarely exceeds 5 percent; fluorite is present locally. Anomalous values of lead and zinc suggest the presence of sphalerite and galena (table 2). Medium- to

[1]Arabian Shield Development Corporation, P.O. Box 1516, Jeddah 21441, Saudia Arabia.
[2]WGM, Inc., P.O. Box 100059, Anchorage, Alaska 99510.

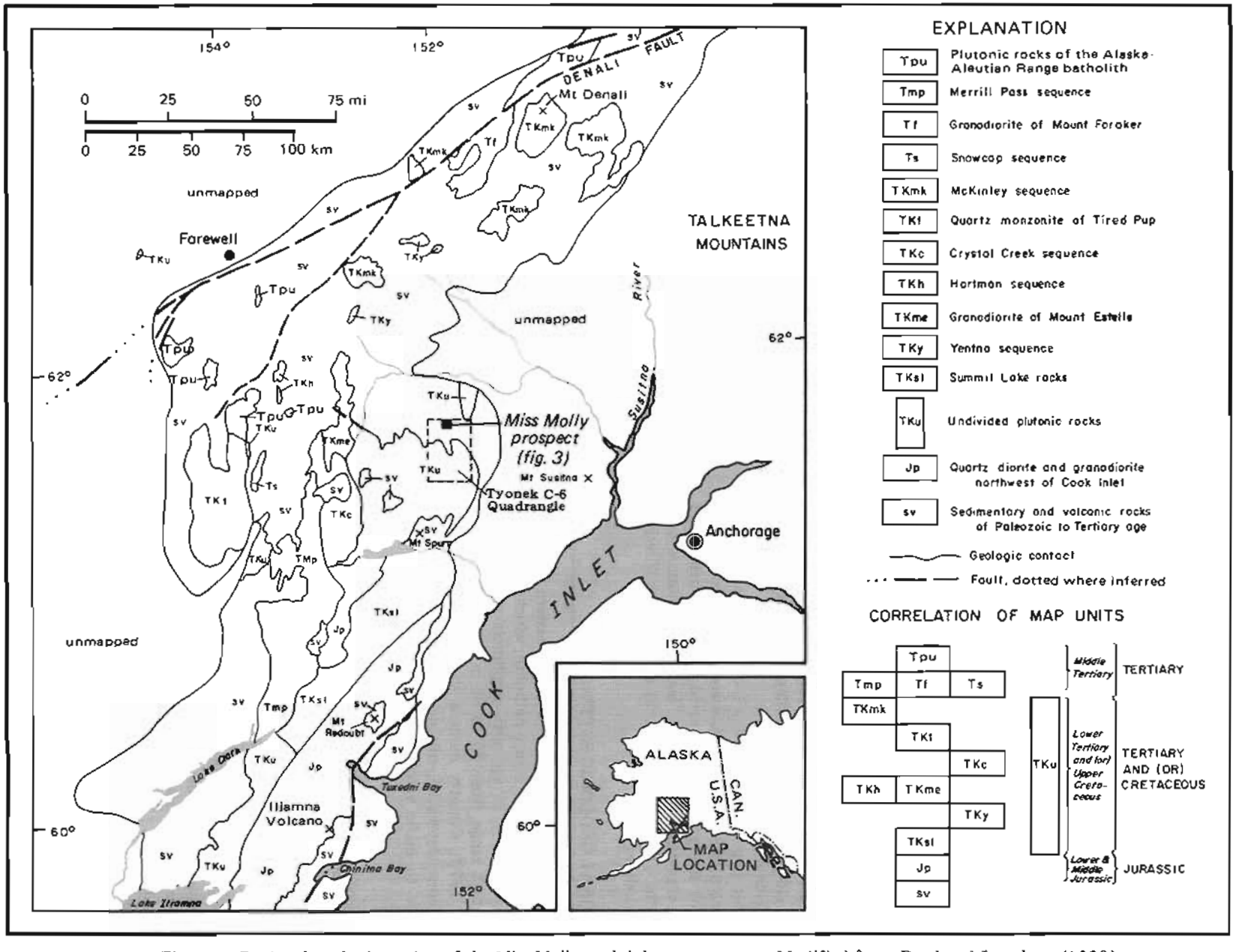

Figure 1. Regional geologic setting of the Miss Molly molybdenum prospect. Modified from Reed and Lanphere (1973).

Figure 2. View west of the prospect. Trimble River mineralized zone is exposed in the prominent outcrops in the center of the photo. The West zone is along a straight creek in the upper left corner.

coarse-grained molybdenite is present in most veins and is commonly concentrated along one wall of the vein or in a single band of quartz within the vein. Molybdenite 'paint' on fracture surfaces was observed rarely. Molybdenite occurs in veins over most of the Trimble River zone, but is most abundant in the northern part of the zone. The molybdenite content of individual veins appears to increase to the southeast.

The West mineralized zone is an area of veining and erratic alteration that is exposed for at least 1,500 ft along a southeast-flowing tributary of the Trimble River. Numerous mineralized veins strike north-northeast across the overall trend of the zone, which parallels the tributary valley. Mineralization consists of pyrite and molybdenite in vein quartz and as local disseminations in granite. A 10- to 70-ft-wide strongly altered and highly veined area near the southeastern end of the zone is associated with a 50- to 75-ft-thick granite dike that intrudes both the main phase of the stock and the country rock to the south.

Hydrothermal alteration occurs as selvages adjacent to quartz veins and shears. Northwest-trending quartz veins and fractures in the Trimble River zone display yellow-weathering sericite-pyrite alteration selvages up to 12 in. wide. The alteration selvages appear wider in

Table 1. *Whole-rock analysis, sample 70, Miss Molly prospect.*[a]

Oxide/Element	Content (wt %)
SiO_2	80.9
Fe_2O_3	3.1
Al_2O_3	8.9
CaO	0.15
MgO	0.1
Na_2O	1.4
K_2O	2.8
MnO	0.02
TiO_2	0.2
P_2O_5	0.03
S	0.23
Total	97.83

[a] Atomic-absorption and colorimetric analyses by Bondar-Clegg & Company, Ltd., 130 Pemberton Ave., North Vancouver, B.C., Canada V7P 2R5.

Table 2. *Rock geochemical data, Miss Molly prospect (ppm, except Au in ppb).*[a]

Sample	Type	Description	Mo	Cu	Pb	Zn	W	Sn	Ag	Au
12	15-ft chip	Granite with NW-trending quartz veinlets (some with molybdenite 'paint') 3-18 in. apart	196	15	18	73	13	<5	0.2	10
14	Grab	Contact between granite and hornfelsed siltstone	284	57	10	288	3	<5	0.4	10
21	60-ft chip	Fresh granite with 6-in.-wide, NW-trending, molybdenite-bearing quartz veins spaced regularly at 7- to 11-ft intervals	630	18	72	242	4	<5	2.5	40
22	60-ft chip	Weakly altered granite with 3- to 4-in.-wide quartz-pyrite-molybdenite veins with 1- to 3-in.-wide sericitic alteration selvages	490	1	39	71	6	<5	1.6	15
23	6-ft chip	Strongly altered granite with several quartz-pyrite-molybdenite veins	490	13	57	115	4	<5	4.6	50
24	40-ft chip	Weakly altered granite with manganese-oxide stain and numerous small, discontinuous quartz veins	20	3	9	42	5	<5	0.2	20
26	15-ft composite grab	Strongly altered granite near intersecting shear and fracture sets	34	1	3	20	10	<5	0.2	5
27	105-ft chip	Altered granite with numerous NW-trending quartz veins, fractures, and shears	276	4	31	1570	6	<5	1.4	100
28	105-ft chip	Weakly altered granite with NW-trending, molybdenite-bearing quartz veins	775	8	320	400	6	<5	11	30
29	45-ft chip	Relatively unaltered granite with NW-trending quartz veins; sparse molybdenite	82	3	13	98	5	6	0.4	<5

35	Grab	Fresh granite with partly altered biotite; minor manganese stain	6	<1	8	35	4	<5	0.2	<5
36	Composite grab	Fresh granite with numerous thin, crosscutting quartz veinlets; minor pyrite	72	<1	10	31	4	<5	0 2	10
37	Grab	Fresh granite; local disseminated molybdenite in outcrop	19	1	4	32	3	<5	0.2	<5
62	Talus composite	Weakly altered granite	420	2	8	22	2	8	0.2	<5
63	Composite grab	Altered granite with disseminated pyrite	1820	5	18	41	8	14	0.4	35
64	Composite grab	Weakly altered granite; disseminated pyrite and molybdenite	970	<1	6	20	9	<5	0.5	10
65	Composite grab	Sericitically altered granite with irregular quartz veinlets	173	6	4	5	8	<5	0.7	35
66	Composite grab	Altered granite with quartz veinlets and disseminated molybdenite	220	<1	4	20	11	<5	0 2	10
67	Composite grab	Fresh and altered granite with thin quartz veins; local molybdenite	82	3	3	10	9	8	0 2	<5
68	Composite grab	Unaltered granite	42	3	3	24	9	6	0.2	<5
69	Composite grab	1-ft-thick quartz-molybdenite vein with 1 ft of sericitized granite on each side of vein	1820	1	13	6	15	7	0 6	10
70	4-ft composite grab	Altered and veined zone in unaltered granite	3800	21	30	23	5	25	0.6	16
71	Composite grab	Sample from altered and veined zone 10 to 65 ft wide and 300 ft long	425	1	7	16	6	<5	0.4	40

[a] Analysis by Bondar-Clegg & Company, Ltd., 130 Pemberton Ave., North Vancouver, B.C., Canada V7P 2R5.
Mo, Cu, Pb, Zn, Ag (atomic absorption)
Au (atomic absorption, fire assay)
Sn (X-ray fluorescence)
W (colorimetry)

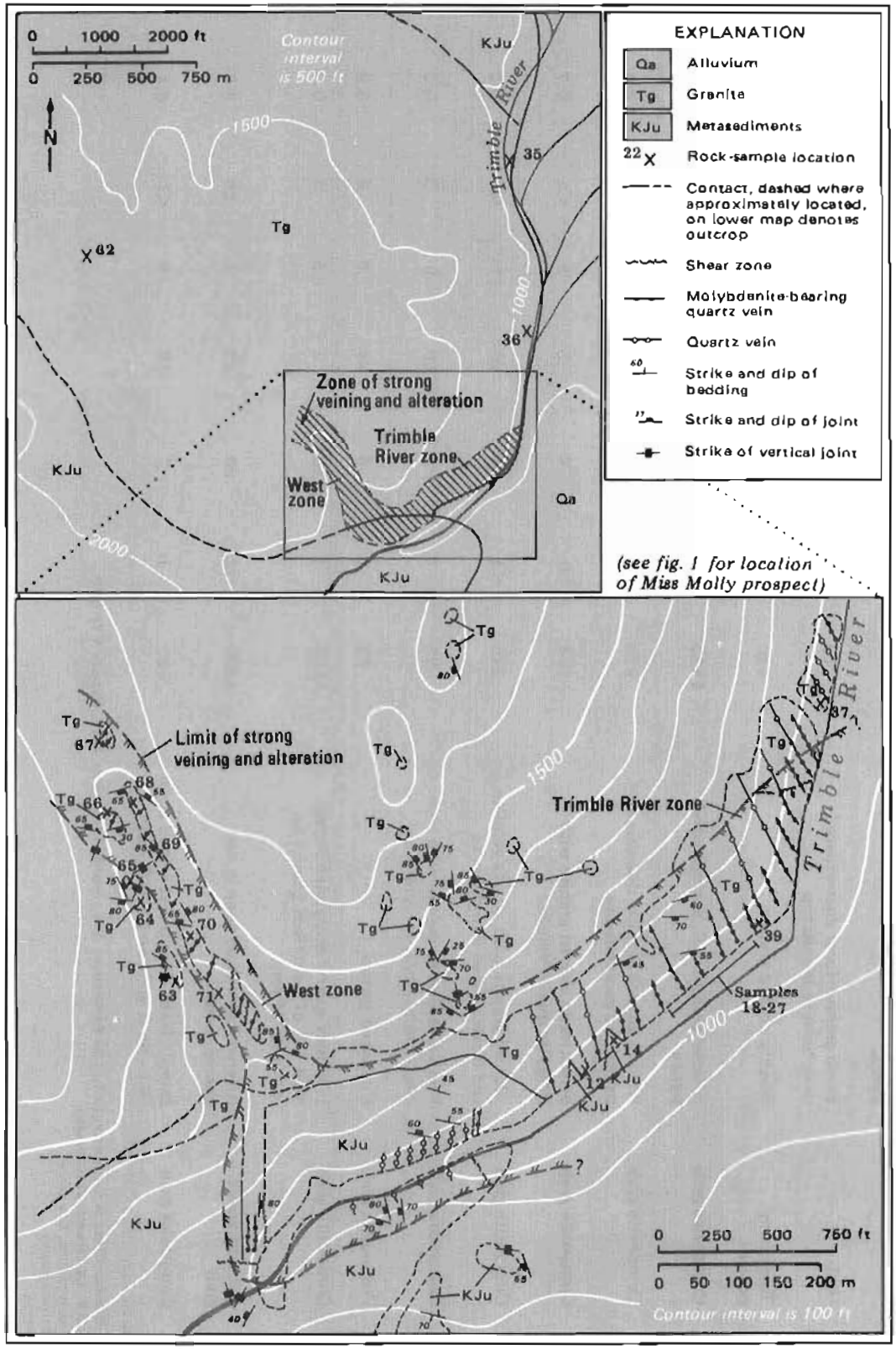

Figure 3. Geology of the Miss Molly molybdenum prospect. Top: General geology of property; bottom: detailed geology of mineralized zones.

Figure 4. Molybdenite-bearing quartz vein with sericite-pyrite alteration selvage.

the central part of the zone and in places coalesce to form pervasively altered blocks several tens of feet across. Clay and possibly alunite of primary or secondary origin also occur in pervasively altered areas. Most alteration in the Trimble River zone is associated with northwest-trending veins and shears, but in more pervasively altered areas, it is also controlled by shear and joint sets that trend N. 40°-60° E. and dip 40° to 80° SE. Alteration in the West zone is associated with northeast-trending fractures and veins. Although sericite-pyrite alteration is generally controlled by individual veins and fractures, much of the rock in the two mineralized zones and in surrounding parts of the stock is affected by a weak but widespread alteration that is characterized by slight to partial degradation of feldspars and the presence of disseminated red-brown hematite(?).

Chip samples along 391 ft of the most strongly altered part of the Trimble River zone (samples 21-28, table 2) have a weighted average of 483 ppm molybdenum (0.08 percent MoS_2). Rock sampling is less complete to the north and south, but suggests a decrease in grade. The arithmetric average of nine composite grab samples (samples 63-71, table 2) from the West zone is 1,039 ppm molybdenum (0.14 percent MoS_2). However, because these are reconnaissance samples, they may not accurately represent the average grade of the West zone. A sample of weakly altered granite (sample 62, table 2) taken 4,000 ft northwest of the West zone contains 420 ppm molybdenum and may indicate the presence of other mineralized areas.

CONCLUSIONS

Molybdenum mineralization at the Miss Molly prospect is in a structurally controlled alteration-mineralization system of moderate size and grade. The molybdenite-bearing quartz veins are secondary dilatant features related to structural elements that control the two large mineralized and altered zones. The prospect is not a classic stockwork-molybdenum type, but the alteration and mineralization may indicate a larger, more strongly altered and mineralized system elsewhere in the stock. This possibility is supported by the presence of a thick, late-stage granite dike associated with alteration and mineralization in the West zone, possibly from a subjacent late-stage silicic plug.

ACKNOWLEDGMENTS

We thank Don and Virginia Hawick for permission to publish the data in this paper. C.G. Bigelow, President of WGM, Inc., for his advice and encouragement, and Len Nelson for preparing the figures. This paper benefited greatly from review by Jason Bressler of WGM, Inc., and by T.K. Bundtzen and T.E. Smith of DGGS.

REFERENCES CITED

Berg, H.C., and Cobb, E.H., 1967, Metalliferous lode deposits of Alaska: U.S. Geological Survey Bulletin 1246, 254 p.

Cleveland, Gaylord, Fernette, Gregory, and Ruzicka, Joseph, 1979, Report on preliminary examination, Miss Molly property, August 19-25, 1979: Anchorage, WGM, Inc., unpublished private report, 71 p.

Hawkes, H.E., and Webb, J.S., 1962, Geochemistry in mineral exploration: New York, Harper and Row, 415 p.

Hollister, V.F., 1978, Geology of the porphyry copper deposits of the Western Hemisphere: New York, American Institute of Mining, Metallurgical, and Petroleum Engineers/Society of Mining Engineers, 219 p.

Magoon, L.B., Adkison, W.L., and Egbert, R.M., 1976, Map showing geology, wildcat wells, Tertiary plant fossil localities, K-Ar age dates, and petroleum operations, Cook Inlet area, Alaska: U.S. Geological Survey Miscellaneous Geological Investigations Map I-1019, scale 1:250,000, 3 sheets.

Reed, B.L., and Lanphere, M.A., 1973, Alaska-Aleutian Range batholith: Geochronology, chemistry, and relation to circum-Pacific plutonism: Geological Society of America Bulletin, v. 84, p. 2583-2610.

GLACIAL GEOLOGY OF THE MT. PRINDLE AREA, YUKON-TANANA UPLAND, ALASKA

By F.R. Weber[1] and T.D. Hamilton[2]

INTRODUCTION

The Mt. Prindle area, a highland underlain by resistant granitic rock, is situated 85 km northeast of Fairbanks within the Yukon-Tanana Upland of east-central Alaska. Mt. Prindle is located 16-19 km northwest of the Steese Highway, from which it is accessible via mining roads and trails that lead into the upper courses of its radiating valley system (fig. 1). Mt. Prindle (elevation 1,611 m) is in the center of a 300-km^2 glaciated highland. Ridges that rise to more than 1,200 m are separated by valleys that have been scoured to depths of 500-600 m. Most of the area is above timberline.

The highest parts of the Mt. Prindle area are underlain by an elongate, northeast-trending, 50-km^2 granitic pluton (fig. 2). Tourmaline- and topaz-bearing porphyritic biotite granite has intruded the crystalline schists of the Yukon-Tanana Upland (Holm, 1973). These schists contain mineral assemblages of the lower greenschist facies, but within 1 km of the granitic contact they have been upgraded as high as upper hornblende-hornfels facies. The pluton, which yielded K-Ar ages of 58-56 m.y. (Holm, 1973), is cut by major northeast-striking wrench faults.

The Mt. Prindle area exhibits dramatic evidence for Pleistocene glaciation. Deep cirques occupy the heads of radiating 9- to 11-km-long U-shaped troughs that change abruptly downvalley into V-shaped canyons. Sharp, narrow arêtes between smooth cirque headwalls contrast with nearby unglaciated uplands that exhibit tors, cryoplanation terraces, and other nonglacial erosional features. Evidence for glaciation in the Mt. Prindle area was reported by Saunders (1960), who noted cirques and cols at valley heads and described the striking U-shaped valley of American Creek with its faceted spurs and hanging tributaries (fig. 3). Former glacier limits were later mapped from aerial photographs by Péwé and others (1967), who found evidence for two separate glacial advances in each of six valleys. Their map emphasizes the unique character of Mt. Prindle, which is the only mountain mass in the western Yukon-Tanana Upland to exhibit extensive multiple ice advances.

This study originated in overflights and ground traverses around Mt. Prindle during the 1970s during several other field projects. Our concepts of the Mt. Prindle glacial record were tested and refined during a 3-day helicopter-supported field study in July 1980.

[1]U.S. Geological Survey, Box 80586, Fairbanks, Alaska 99708.
[2]U.S. Geological Survey, 4200 University Drive, Anchorage, Alaska 99508-4667.

GLACIAL SEQUENCE

The six valleys that radiate from Mt. Prindle show evidence for four separate Pleistocene glacial advances. From oldest to youngest, these informally are termed the Prindle, Little Champion, American Creek, and Convert advances. The three youngest advances are associated with modern valley heads and upland terrain features; the oldest ice advance originated from ancient uplands around Mt. Prindle that may have been strongly modified by subsequent erosion.

Prindle Glaciation

Evidence for the Prindle glaciation consists primarily of granite-boulder erratics up to 2.2 m diam on valley floors at the downvalley limits of the U-shaped troughs that radiate from Mt. Prindle (table 1). Erratic boulders that are eroding from the scarps of stream terraces in some localities have evidently undergone repeated episodes of erosion and redeposition since their initial emplacement by glacier ice. Many redeposited boulders have planar-fractured faces that may have resulted from deep weathering along joint planes prior to their most recent exposure. Lateral ice margins farther up the valleys (fig. 2) are suggested by the upper limits of glacial facets, by rare benchlike features that may be moraine remnants, and by sparse patches of probable till.

The Prindle glaciation evidently was followed by a long period of erosion that considerably modified the upland topography around Mt. Prindle. The floors of the upper valleys of Nome and Hope Creeks were not glaciated during younger ice advances and bear deep stream incisions into bedrock; their lower walls are buried by talus that has been modified by at least one episode of rock-glacier activity. Ridge crests and upper valley sides exhibit both numerous tors (fig. 4) and extensive cryoplanation terraces that have formed since valley walls were steepened by glacial erosion during Prindle time. The upper valleys of Champion, Little Champion, Convert, and American Creeks have been extensively modified by the enlargement of cirques during younger glaciations, and valley heads dating from the Prindle ice advance have been obliterated. Headward

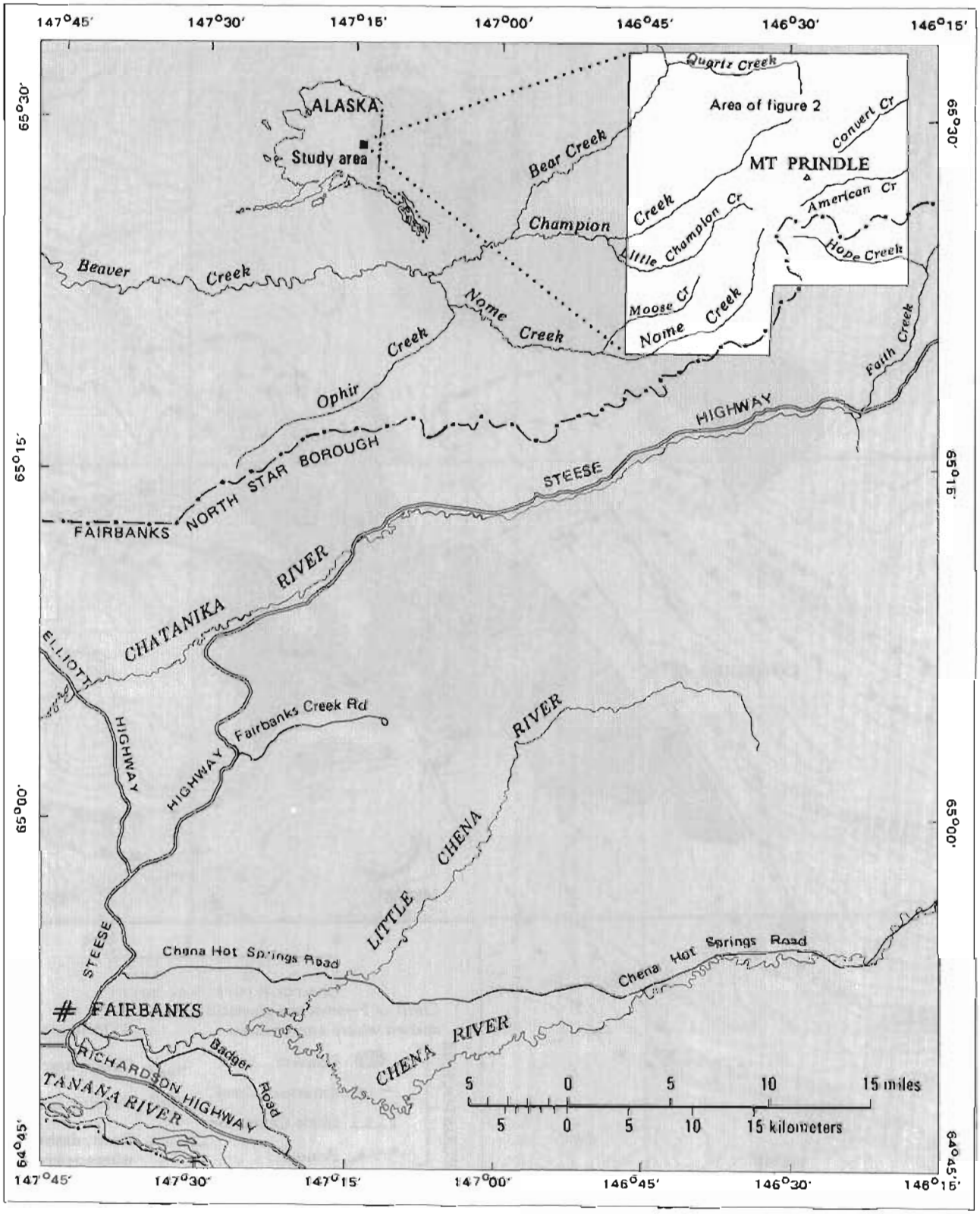

Figure 1. Mt. Prindle area, east-central Alaska.

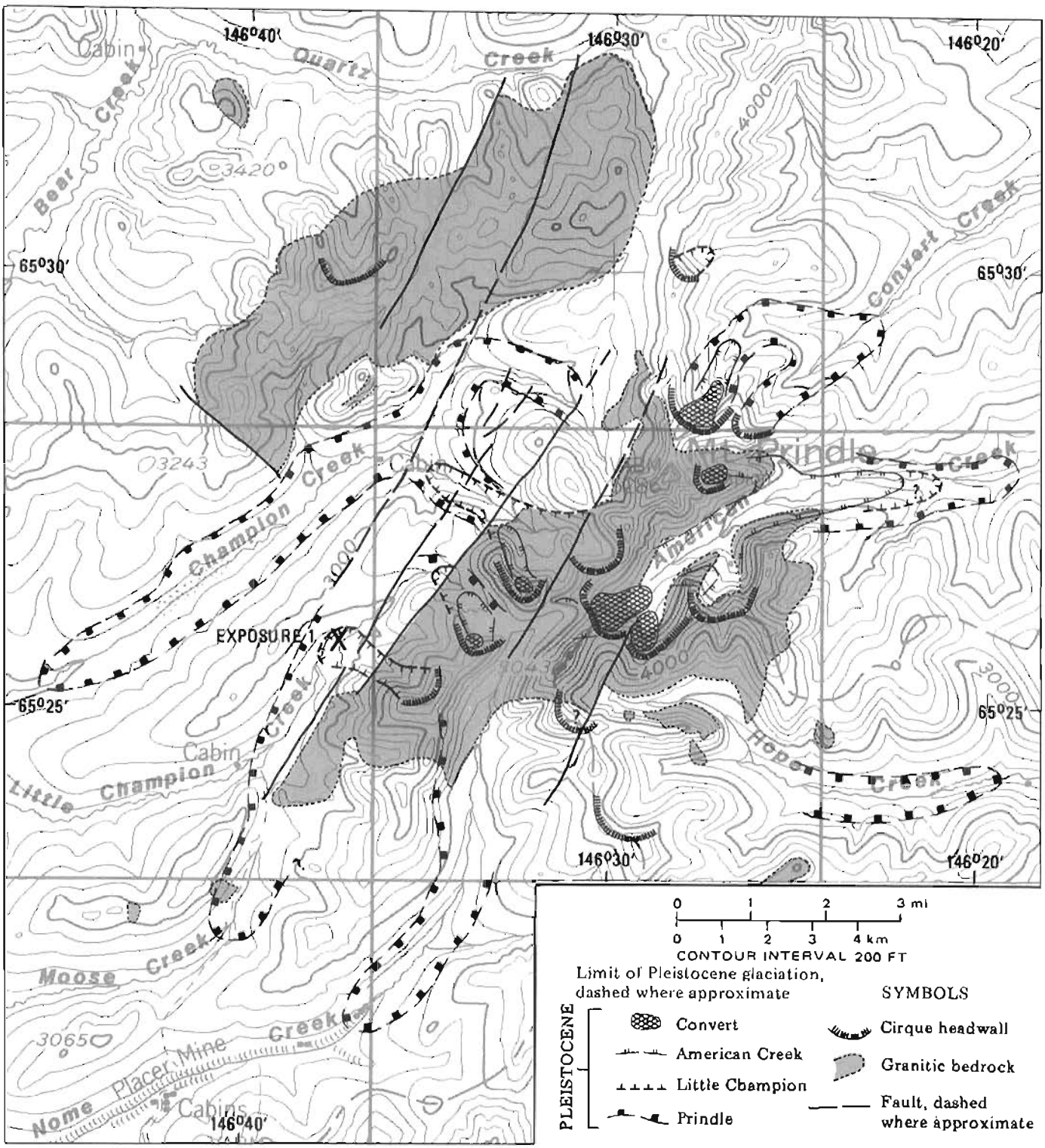

Figure 2. Cirques, radiating valleys, and former glacier limits in the Mt. Prindle area, east-central Alaska.

Table 1. *Downvalley limits of ice advances of Prindle age.*

Drainage	Elevation (m)	Distance from present valley head (km)	Maximum measured size of granite erratics (cm)
Convert	725	4.8	137 x 60 x ?
American	700	9.2	170 x 170 x 70+
Hope	650	10.1	100 x 60 x 50[a]
Nome	710	11.3	210 x 160 x 120
Moose	725	7.2	No data
Champion	600	15.3	220 x 200 x 60+

[a]Measured on upstream end of midchannel bar. Probably moved by modern stream during flood stage.

erosion by Little Champion Creek pirated the upper course of Moose Creek, leaving a large abandoned glacial trough to mark the former position of an ice tongue in the valley of Moose Creek.

Little Champion Glaciation

The Little Champion ice advance is named informally for Little Champion Creek, where till exposed in a deep (37.5 m) river cut (exposure 1, fig. 2) marks the outer limit of a small ice lobe that extended into the valley center from a tributary valley. The till, which has an exposed thickness of 22 m (fig. 5), consists dominantly (95 percent) of subrounded granite cobbles and boulders in a matrix of dark-yellowish-brown (10YR 4/4), poorly sorted, arkosic silty sand. Angular chips of schist and quartzite also are present. All clasts are weathered, and highly weathered stones disintegrate to grus just above the base of the exposed till. The basal 15.5 m of the river bluff is covered by a colluvial apron of angular phyllitic schist fragments that overlie schistose bedrock.

Ice advances of Little Champion age in the valleys of Little Champion and Champion Creeks eroded and widened the floors of tributary valleys that had been incised by streams following the Prindle glaciation. Comparable ice advances evidently did not occur in the valleys of Hope or Nome Creeks or in the south fork of Convert Creek, and any glacial deposits in the north fork of Convert Creek were probably buried by a later, more extensive ice advance. A possible ice limit in the valley of American Creek is indicated by lateral-moraine remnants of deeply oxidized granite boulders that extend along the north flank of the ridge that separates its two principal branches (fig. 2). The end moraine may have been destroyed by erosion near the confluence of the two streams.

American Creek Glaciation

The most extensive ice advance after the Little Champion glaciation occurred in the valley of American Creek. A valley glacier extended 9.5 km northeast from Mt. Prindle, where it was fed by four north- to east-facing cirques (fig. 2). The glacier built a terminal moraine with distinct outer and inner ridges. The outer ridge is largely overlapped by a solifluction apron that extends from the lower valley side, and the inner moraine has a more pronounced, 10-m-wide crest that

Figure 3. View southwest upvalley of American Creek, showing U-shaped cross profile with truncated ridge spurs. Photograph by F.R. Weber, July 17, 1979.

Figure 4. View north toward tors on glaciated surfaces of Prindle age near head of Hope Creek. Photograph by T.D. Hamilton, August 1972.

Figure 5. Oxidized till above bedrock exposed in east-facing bluff along Little Champion Creek. Photograph by F.R. Weber, July 10, 1980.

Figure 6. Deeply etched (by weathering along joint planes) granite boulders on moraine of American Creek age near head of Champion Creek. Photograph by F.R. Weber, July 10, 1980.

stands 2-3 m above the hummocky drift surface. A small pond between the two ridges is partly enclosed by solifluction deposits, and organic sediments are exposed around its entire rim. The pond depression may be a kettle derived from melting glacier ice, but probably originated from thawing of ice-rich permafrost. Rocks exposed on the moraine surface are predominantly granite, with a few subangular quartzite boulders. Most stones have been reduced to masses of angular rubble, and the few granite boulders that remain on the surface are deeply oxidized and have been etched along joint planes to depths of about 4 cm. A pit dug into the inner moraine exposed a well-developed podzolic soil profile with a 4-cm-thick, ashlike, gray, leached A_2 horizon above 25 cm of strongly oxidized, dark-reddish-brown, silty, stony sand. The moraine has been incised by American Creek, and terrace deposits that stand 21.6 m above the modern stream level downstream from the moraine are composed of very sandy, pebble-cobble gravel that has been strongly oxidized to reddish brown (5YR 4/4) through its upper 20-25 cm.

Smaller moraines of comparable age occur at 900-1,100 m elevation within 1-2 km of cirque headwalls at the heads of Convert, Champion, and Little Champion Creeks. The moraines are much more bouldery than those in the valley of American Creek, but surface boulders are strongly weathered, embedded in grus, and surrounded by soils that have been oxidized to dark or reddish brown. The terminal moraine in Convert Creek has been beveled by stream erosion to form a bench 14 m above the modern creek. Granitic boulders on the moraine at the head of Champion Creek have been etched as deeply as 20-30 cm along fracture planes (fig. 6), and associated outwash has been incised to depths of more than 9 m. The moraine at the head of Little Champion Creek is the most subdued, with flanking slopes of 7-8 degrees. Its surface also bears strongly weathered granite boulders embedded in grus. The associated cirque headwall is weathered and partly vegetated, with stabilized talus along its base.

Convert Glaciation

During the final episode of glacier expansion, small ice bodies and rock glaciers developed in six northeast-facing cirques at the heads of Convert, American, Champion, and Little Champion Creeks. These features were less than 1 km long, and none extended below 1,025 m elevation.

The type locality of the largest moraine of the Convert glaciation is in a cirque at the head of American Creek 3 km south of Mt. Prindle. The term 'Convert' (from an adjoining valley that also bears moraines of this age) is used to distinguish the younger glaciation from the older American Creek event. The moraine has an irregular surface with a steep (19-degree) frontal slope and only small, local patches of solifluction debris. It is flanked on the southeast by a boulder-floored meltwater channel. Abundant granite boulders are little weathered and emit a sharp metallic sound when struck with a hammer. Buried clasts are surrounded by thin (1- to 2-cm-thick) grus halos, but freshly broken surfaces generally lack oxide discolorations. Soils are immature and consist typically of thin (2- to 4-cm-thick) organic mats and shallow (20-cm-deep) accumulations of brown loess above unaltered, gravelly till. The moraine has been narrowly (30 to 40 m wide) incised to a depth of 11 m by the creek. Large, vegetated talus cones and fans of combined fluvial and colluvial origin occur downvalley from the moraine, whereas only smaller cones of fresh talus occur upvalley. The large stabilized forms probably evolved as periglacial features during the Convert glaciation because comparable deposits are not forming in the Mt. Prindle area today.

The rubble deposit at the head of Convert Creek

lacks lateral- and terminal-moraine forms and is most bulky where fed by the largest talus cones from the cirque headwall. Small streams flow around both flanks, but the axial stream that generally incises cirque moraines is absent. Surface stones are strongly weathered and resemble the weathered clasts of American Creek age more than those of the younger glaciation. This deposit probably represents a rock glacier that developed during the Convert glaciation and incorporated older rubble during its advance.

Smaller, stable rock glaciers occur at the bases of cirque headwalls at the heads of Champion and Little Champion Creeks. These features resemble the talus-derived, lobate rock glaciers described by White (1976). They are within end moraines of American Creek age; are stable, lichen-covered, and partly vegetated; and probably formed as periglacial features during the Convert glaciation.

SUMMARY AND DISCUSSION

The six major valley systems of the Mt. Prindle area record four principal glacial advances. During the oldest (Prindle) advance, glaciers radiated outward from a central source area that has since been largely eroded. Ice tongues were most extensive in southern and western valley systems and least extensive to the northeast—a relationship opposite to that of later glaciations—perhaps implying different regional or local climatic controls. Perhaps the ice tongues of Prindle age radiated from a central ice cap that was nourished by heavy snowfall from westerly and southerly winds. The Alaska Range may have been less of a barrier to maritime air masses during early Pleistocene time than it is today. The Prindle glaciation was followed by a very long interval of erosion, when major streams were pirated and streams deeply incised most of the glaciated valley floors.

During each of the three younger glaciations, ice bodies originated in the same cirques and followed identical courses through valley systems that differ little from the modern drainage of the Mt. Prindle area. Valley floors scoured by ice tongues of Little Champion age have been only slightly incised by modern streams, and cirque and valley walls show little alteration by cryoplanation and other periglacial processes. The interval between the Prindle and Little Champion ice advances may have been longer than the total duration of all the subsequent glacial advances and intervals.

Glaciers of Little Champion, American Creek, and Convert age were successively less extensive and increasingly limited to cirques with northeastern orientations. Some cirques were abandoned entirely during younger, less extensive glaciations; others supported rock glaciers whose activity may have coincided with times of general ice advance. Although we lack firm

Table 2. *Suggested correlation of Mt. Prindle glacial phases with other Alaskan glacial and sea-level records. Data from Péwé (1975), Carter (1980), Hamilton (1982), and Hamilton and Hopkins (1982).*

Mt. Prindle area	Alaska Range (Delta River Valley)	Alaska Range (Nenana River Valley)	Brooks Range	Approximate age (yr B.P.)
Convert	Donnelly	Riley Creek	Walker Lake	
- - - - - - - - - -	- - - - - - - - - -	- - - - - - - - - -	- - - - - - - - - -	Middle Wisconsinan (40,000)
American Creek	Delta	Healy	Itkillik	
- - - - - - - - - -	- - - - - - - - - -	- - - - - - - - - -	- - - - - - - - - -	Pelukian (125,000)
Little Champion	- - -	'Lignite Creek'	Sagavanirktok River	
XXXXXXXXXX	XXXXXXXXXX	XXXXXXXXXX	XXXXXXXXXX	Kotzebuan (>175,000); <250,000)
Prindle	Darling Creek	Browne erratics	Anaktuvuk River	
XXXXXXXXXX	XXXXXXXXXX	XXXXXXXXXX	XXXXXXXXXX	Anvilian (>700,000 <1,800,000)
???	Tertiary tillites(?)	Pre-Browne erratics	Gunsight Mountain erratics	

- - - Indicates minor erosion interval.
XXX Indicates major erosion interval.

dates on the glacial episodes, our measurements on weathering rates, soil development, slope modification, and stream incision suggest that approximately comparable intervals of time separated the three youngest ice advances. These data also allow provisional correlation with similar glacial successions described elsewhere in central and northern Alaska (table 2).

Placer gold was discovered about 1898 on Faith, Hope, and Charity Creeks. Subsequently, gold mining has been active on nearly all creeks that radiate from Mt. Prindle. The origin of the gold in this area is not clearly understood, but it probably is related to Tertiary dikes, veins, and small hypabyssal intrusions rather than to the main Mt. Prindle intrusion. To the best of our knowledge, no gold is being mined within the area that once was occupied by glaciers. These ice bodies probably eroded alluvial placer deposits that had developed in the upper parts of each valley so that gold presently is found only below the maximum glacial extents.

ACKNOWLEDGMENTS

We thank R.A. Combellick and R.D. Reger (DGGS) for their helpful reviews.

REFERENCES CITED

Carter, L.D., 1980, Tertiary tillites(?) on the northeast flank of Granite Mountain, central Alaska Range, *in* Short notes on Alaskan geology - 1979-80: Alaska Division of Geological and Geophysical Surveys Geological Report 63, p. 23-27.

Hamilton, T.D., 1982, A late Pleistocene glacial chronology for the southern Brooks Range - stratigraphic record and regional correlations: Geological Society of America Bulletin, v. 93, no. 8, p. 700-716.

Hamilton, T.D., and Hopkins, D.M., 1982, Correlation of northern Alaskan glacial deposits - a provisional stratigraphic framework, *in* Coonrad, Warren, ed., The United States Geological Survey in Alaska: Accomplishments during 1980: U.S. Geological Survey Circular 844, p. 15-18.

Holm, Bjarne, 1973, Bedrock geology and mineralization of the Mount Prindle area, Yukon-Tanana Upland, Alaska: Fairbanks, University of Alaska unpublished M.S. thesis, 55 p.

Péwé, T.L., 1975, Quaternary geology of Alaska: U.S. Geological Survey Professional Paper 835, 145 p.

Péwé, T.L., Burbank, Lawrence, and Mayo, L.R., 1967, Multiple glaciation of the Yukon-Tanana Upland, Alaska: U.S. Geological Survey Miscellaneous Geologic Investigations Map I-507, scale 1:500,000, 1 sheet.

Saunders, R.H., 1960, Notes on glaciation in the Circle Quadrangle: Unpublished Alaska Territorial Department of Mines Miscellaneous Report 50-4, 4 p.

White, S.E., 1976, Rock glaciers and block fields, review and new data: Quaternary Research, v. 6, no. 1, p. 77-97.

STAFF

Ross G. Schaff, State Geologist
W.W. Barnwell, Deputy State Geologist

Administrative Services

.S.A. Aasland, Clerk typist
.P.L. Coonrod, Secretary
.D.R. Debenham, Clerk typist
.R.R. Jensen, Administrative officer
.E.M. Lamey, Administrative assistant
.C.L. Mahan, Accounting technician
.R.J. Michels, Supply technician
.D.J. Mursch, Clerk typist
.J.N. Newgaard, Accounting technician
.K.E. Ohlund, Clerk typist
.V.L. Reger, Geological assistant
.J.E. Richards, Clerk typist
.N.D. Sizemore, Clerk typist
.B.A. Syvertson, Clerk typist
.J.L. Weir, Clerk typist
.M.E. Wright, Clerk typist

Archaeology

.R.G. Dixon, Archaeologist
.D.E. Gibson, Archaeologist
.C.E. Holmes, Archaeologist
.S.L. Klingler, Archaeologist
.J.D. McMahan, Archaeologist
.C.W. Mishler, Historian
.D.R. Reger, Archaeologist
.R.D. Shaw, Archaeologist

Data Processing

.N.W. Crosby, Operations research analyst
.B.S. Hurtig, Analyst programmer
.K.M. Rhoades, Analyst programmer
.B.A. White, Operations research analyst

Engineering Geology

.J.N. Davies, Geologist
.R. Ranken, Geologist
.J.W. Reeder, Geologist
.C.A. Ulery, Geological assistant
.R.G. Updike, Geologist

Geochemistry

.M.R. Ashwell, Minerals laboratory technician
.J.D. Blum, Geological assistant
.K.B. Faris, Chemist
.M.K. Polly, Minerals laboratory technician
.N.C. Veach, Chemist
.M.A. Wiltse, Chemist

Geologic Mapping

.D.D. Adams, Geological assistant
.M.D. Albanese, Geologist
.T.K. Bundtzen, Geologist
.L.E. Burns, Geologist
.R.A. Combellick, Geologist
.J.E. Decker, Geologist
.J.T. Dillon, Geologist
.W.G. Gilbert, Geologist
.D.R. Hickmott, Geological assistant
.J.T. Kline, Geologist
.K.L. Krause, Geologist
.T.A. Little, Geologist
.G.D. March, Geologist
.G.H. Pessel, Geologist
.S.E. Rawlinson, Geologist
.R.D. Reger, Geologist

Geologic Mapping (con.)

.R.R. Reifenstuhl, Geological assistant
.M.S. Robinson, Geologist
.T.E. Smith, Geologist

Information Services

.C.L. Daniels, Publications specialist
.G.M. Laird, Cartographer
.L.F. Larson, Publications specialist
.R.A. Mann, Clerk
.K.S. Pearson, Cartographer
.L.C. Schell, Cartographer

Minerals & Energy Investigations

.J.G. Clough, Geologist
.G.R. Eakins, Geologist
.S.A. Liss, Geological assistant
.L.L. Lueck, Geologist
.R.D. Merritt, Geologist
.M.A. Moorman, Geologist
.R.J. Motyka, Geologist
.C.J. Nye, Geologist

Oil and Gas

.D.L. Bertossa, Geological assistant
.J.J. Hanson, Geophysicist
.E.E. Harris, Geological assistant
.M.W. Henning, Geologist
.S.A. Jacques, Cartographer
.R.W. Kornbrath, Geologist
.D.L. Krouskop, Geophysicist
.W.M. Lyle, Geologist
.D.L. McGee, Geologist
.J.F. Meyer, Geophysicist
.C.G. Mull, Geologist
.M.E. Pritchard, Cartographer
.T.N. Smith, Geologist
.S.M. Weum, Geophysicist
.B.K. Wilson, Geological assistant

Resource Analysis

.E.E. Becia, Natural resource manager
.R.M. Bennett, Natural resource manager
.M.S. Christy, Geologist
.K.H. Clautice, Geological assistant
.G. Dickinson, Natural resource officer
.G. Finch, Data entry clerk
.E.L. Jenks, Analyst programmer
.T.G. Johnson, Data control specialist
.J.J. Jurgens, Analyst programmer
.L.P. White, Operations research analyst
.M.J. Wibbenmeyer, Natural resource manager

Water Resources

.R.D. Allely, Hydrologist
.S.J. Carrick, Hydrologist
.E.J. Collazzi, Hydrologist
.L.L. Dearborn, Hydrologist
.M.G. Ingram, Hydrologist
.R.W. Ireland, Hydrologist
.W.E. Long, Hydrologist
.S.F. Mack, Hydrologist
.M.A. Maurer, Hydrologist
.G.A. McCoy, Hydrologist
.J.A. Munter, Hydrologist


Alaska Department of
NATURAL
RESOURCES